NOVEL SUSTAINED RELEASE BIODEGRADABLE DRUG DELIVERY SYSTEM FOR TARGETING CHRONIC RHINOSINUSITIS

by

Ankit Parikh

Submitted in partial fulfilment of the requirements
for the degree of Master of Science

at

Dalhousie University
Halifax, Nova Scotia
August 2014

This dissertation is dedicated to my mom, dad, brother, fiancée and my all other family members and friends, who believed in me and always supported me. Thank you for all your love and support.

TABLE OF CONTENTS

LIST OF TABLES

LIST OF FIGURES

ABSTRACT

Chronic rhinosinusitis (CRS) is a condition in which the nasal cavity and the paranasal sinuses become inflammed causing facial pressure, pain, headache, nasal obstruction and thick nasal discharge. CRS severely affects patients' quality of life and it can last for a duration greater than 12 weeks. Nasal sprays are most commonly used for this condition but the duration of action is short. In polypoidal form of CRS, sprays also fail to target the potentially infected anatomic sites. Functional endoscopic sinus surgery (FESS) is a treatment option for patients non-responsive to medical strategies. However, relapses related to infections and inflammations are often encountered setbacks following FESS. To overcome these limitations, sustained release biodegradable drug-eluting nasal implants were developed, which has the potential to be used as adjuncts to FESS to promote wound healing. Several formulations of dexamethasone-loaded poly (lactic-co-glycolic acid) (PLGA) based microparticles were developed using emulsification-solvent evaporation method. The *in vitro* drug release profiles, encapsulation/loading efficiency, surface morphology, mean particle size and size distribution profiles of the formulations were investigated. The results suggested that dexamethasone-loaded PLGA microparticles release the drug in a sustained manner for more than 3 months owing to slow degradation of PLGA. After optimization of suitable formulations, the microparticles were incorporated into an implant or delivery system (sponge and hydrogel). The entrapment efficiency and surface morphology of the implants were subsequently characterized.

LIST OF ABBREVIATIONS USED

CRS	Chronic rhinosinusitis
CRSwNP	Chronic rhinosinusitis with polyps
CRSsNP	Chronic rhinosinusitis without polyps
FESS	Functional Endoscopic Sinus Surgery
DES	Drug-Eluting Stent
PLA	Polylactic acid
PLGA	Polylactic-co-glycolic acid
FDA	US Food and Drug Administration
PVA	Polyvinyl alcohol
DCM	Dichloromethane
GDP	Guanosine 5'-diphosphate
HPLC	High Performance Liquid Chromatography
ACN	Acetonitrile
DMSO	Dimethylsulfoxide
FBS	Fetal Bovine Serum
DMEM	Dulbecco's Modified Eagles Medium
PBS	Phosphate buffered Saline
HBSS	Hanks Balanced Salts Solutions
HEPES	4-(2-hydroxyethyl)-1-piperazineethanesulfonic acid
USP	United States Pharmacopoeia
ICH	International Conference on Harmonization

LOQ	Limit of Quantification
µg/ml	Micrograms per milliliter
$\mu g/cm^2$	Micrograms per square centimeter
µM	Micromolar
µm	Micrometer
AUC	Area Under curve (Peak area)
QC	Quality Control
CV	Co-efficient of Variation
O/W	Oil-in-Water
rpm	Rotations per minute
SEM	Scanning Electron Microscopy
MFI	Micro-Flow Imaging
HCl	Hydrochloric acid
USP	United States Pharmacopoeia
RSD	Relative Standard Deviation
XRD	X-ray diffraction
MW	Molecular weight

ACKNOWLEDGEMENTS

Although only my name appears on the cover of this dissertation, many people contributed to its realization. I owe my gratitude to all those people who have made this dissertation possible and because of whom my graduate experience has been one that I will cherish forever.

My deepest gratitude goes to my advisor, Dr. Remigius Agu. I have been amazingly fortunate to have an advisor who gave me the freedom to explore on my own and at the same time the guidance to recover when my steps faltered. Dr. Agu taught me how to question thoughts and express ideas. His patience and support helped me overcome many crises situations that enabled me to finish this dissertation. It was a great opportunity to do my Masters under his guidance and to learn from his research expertise. I also appreciate the enormous support received from my co-supervisor, Dr. Emad Massoud. His patience, time, ideas and constructive criticism were greatly appreciated. I would like to thank Dr. Pollen Yeung for his comments and suggestions. This project would not have been completed without the support of my thesis advisory and examination committee. In this regard I acknowledge the support received from Dr. Tannis Jurgens. I would like to express my gratitude to the Director, Rita Caldwell, for making my stay in Canada financially possible. Financial support from the Dalhousie Pharmacy Endowment Fund and Capital Health District Authority was of immense help. The Faculty and Administrative staff (Tracy Jollymore, Wanda Dundas and Kate O'brien) were very kind to me and I thank them very much. I am indebted to my colleagues for their valuable suggestions and continuous co-operation throughout my research project.

I wish to express my everlasting thanks to my parents, brother and fiancée without whose inspiration and encouragement this work would never have been completed.

CHAPTER 1 INTRODUCTION

The nose plays a crucial role in airway homeostasis by warming up, humidifying and filtering incoming air. This function may not be possible without the paranasal sinuses. The sinuses, especially the maxillary sinuses are prone to diseases and chronic inflammation. Prior to exploring drug delivery strategies to the sinuses and its challenges, it is important to discuss the anatomy and physiology of the nose and paranasal sinuses, as well as chronic sinusitis, the commonest chronic disease that affects this area.

1.1. Anatomy and physiology of the nose and paranasal sinuses

The paranasal sinuses are air-filled cavities found in the facial bones[1]. These cavities are connected to the nasal cavity to form a complex system at the entrance of the upper airway as shown in Figure 1. This complex unit has highly specific functions,including humidifying, filtering, warming and air conditioning of inhaled air which forms an immunological response against particles in the inspired air, thereby protecting the delicate structures of the lower respiratory system[2,3]. The paranasal sinuses include frontal, maxillary, ethmoid and sphenoid sinuses[3]. The maxillary sinuses are the largest of the sinuses and are located in the cheek, whereas the ethmoid sinuses are located in the anterior base of the skull[2,4]. The frontal and sphenoid sinuses are located in the frontal (forehead)[4] and sphenoid (skull base) bones, respectively[2,4]. The nasal cavity opens anteriorly in the nostrils and connects posteriorly to the nasopharynx. The lateral wall of the nasal cavity is formed by the surfaces of the lacrimal bones and the maxillae and supports the inferior, middle and superior turbinates[2,5]. These turbinates divide the

nasal cavity into the inferior, middle and superior meatus. The middle meatus contains the orifices of the frontal, maxillary and the anterior cells of the ethmoid sinuses. These sinuses drain into the osteomeatal complex. Blockage of the ostium results in inflammation, especially within the maxillary sinuses leading to mucosal swelling and accumulation of secretions.

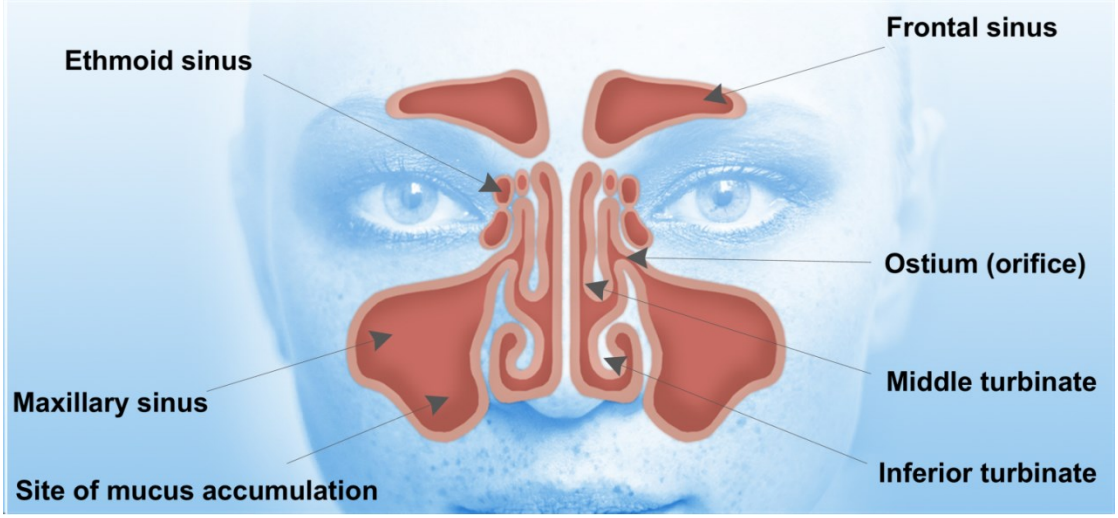

Figure 1 Human facial anatomy showing the location of sinuses.

Inflammation in the paranasal sinuses is often associated with inflammation within the nasal cavity hence the term chronic rhinosinusitis (CRS) is sometimes used to describe the condition. CRS is a clinical syndrome associated with persistent inflammation of the nasal mucosa and paranasal sinuses which encompasses both polypoid (CRSwNP) and non-polypoid (CRSsNP) forms of the disease[6,7,8]. Chronic inflammation of the sinuses results in nasal obstruction, thick nasal discharge, reduction or loss of olfaction and facial pressure or pain[9]. The pathophysiology of CRS is characterized by a diversity of immunological mechanisms involving the T-cells, eosinophilic/neutrophilic inflammation, and airway remodeling. Therefore, CRS with polyps has been frequently associated with asthma[10].

Some CRS patients may require functional endoscopic sinus surgery (FESS) to resolve the condition. Drug-eluting nasal stents/implants can be used as adjuncts to endoscopic sinus surgery to enable better sinus drainage and wound healing.

1.2. Current strategies to deliver drugs to the nasal sinuses and the need for improvement

Management of CRS can be complex, and definitive evidence-based protocols are not currently defined because of the disease heterogeneity, incomplete understanding of its refractory characteristics and differences in individual responses to various interventions[11]. Currently, the initial treatment for uncomplicated CRS is conservative medical therapy, including antibiotics and corticosteroids[12],[13],[14]. Functional endoscopic sinus surgery (FESS) is widely considered to be the standard treatment for medically refractory CRS[7]. Success in outcomes of FESS in patients with CRS with polyps is heavily dependent on reducing postoperative scarring, edema, and crusting that can inhibit natural ciliary function and sinus drainage[15]. Many CRS patients with polyps do not respond well to inhaled steroids and the polyps often re-grow following surgery[1]. Therefore, treatment of CRS with polyps is still an unmet medical need. Also, CRS with polyps arises from prolonged obstruction of the osteomeatal complex, thus leading to mucociliary dysfunction preventing mucous drainage, and failure to clear bacteria from the sinuses[16]. Many drugs used for treating chronic sinusitis are given as nasal sprays or oral formulations. Though, various methods of topical drug delivery such as nasal drops and nasal sprays are generally well accepted, only a few studies have concentrated on intranasal drug distribution[16]. Unfortunately, sprays fail to target potentially affected anatomic sites

such as the maxillary sinus, ethmoid cells or middle turbinate because these areas are occluded from the nasal passage due to inflammation[17]. As CRS is a condition which lasts for a duration longer than 12 weeks, a drug delivery system with prolonged mucosal contact time with local absorption and minimal depletion are often desirable[16,18]. A variety of adjunctive devices have been applied to the sinuses during FESS to keep the middle meatus open, with varying success; these include packing materials, injectable space-filling gels or structured stents[19],[20]. Recent studies have shown that soaking these packing materials with drugs during surgery showed inconsistent results in terms of wound healing, maintenance of ostium (orifice) patency and prevention of polyposis recurrence. Moreover, drug release from nasal packing materials is uncontrolled and inconsistent which may explain the erratic outcome of this treatment strategy. For these reasons, nasal drug-eluting implants with prolonged mucosal contact time which releases the drug locally to the affected site for a prolonged period of time appear to be an option that may assist in solving some of these problems.

1.3. Drug-eluting stents and implants: definition and nomenclature

Stent is defined as a device which is placed into a cavity temporarily to keep it open, promote wound healing and relieve an obstruction[21], whereas FDA defines implant as a device which can be placed into a naturally or surgically formed cavity of the human body in order to remain there for a period of 30 days or more. However, in order to protect public health and depending on the intended application, FDA may also consider that devices placed for shorter periods are also implants[22]. Drug-eluting stents (DESs) or

implants are surgically inserted scaffolds that help in healing the affected tissue by releasing loaded-drug locally and continuously in a controlled manner for the desired period of time[23]. Thus, a stent or an implant is basically a support placed temporarily inside a cavity, duct or a blood vessel to aid healing and/or relieve an obstruction[24]. However, "implant" is a more suitable term to describe drug-eluting nasal devices as CRS being a chronic condition which requires the medical devices to be implanted for greater than 30 days for prolonged drug release. Implants, in general have a wide range of applications, and are used to improve the quality of function, and hence the quality of life of the people who use them[25]. Nasal implants are devices that are inserted in the nose following nasal or paranasal sinus surgery. These devices may be used to locally treat nasal and paranasal infections, inflammations, neoplasm, autoimmune diseases and nasal reconstruction for aesthetic deformities[26]. Nasal implants can also be effectively used for the treatment of sinusitis[27]. Thus, drug-eluting nasal devices release drug-load slowly and continuously from polymer matrices to affected areas in the sinuses or nasal cavities for a prolonged period of time. The major advantage of nasal drug-eluting implants compared to standard nasal sprays is summarized in Figure 2. Following standard nasal sprays, the administered drugs are removed within a few hours by the mucociliary clearance. Little or no drugs are detected within a few hours. In contrast, drug-eluting nasal implants ensure continuous drug release over prolonged period of time to the affected mucosa for CRS treatment. Therefore, nasal sprays that are currently used for refractory CRSwNP treatment[28] not only fail to target the potentially affected anatomic sites[17] but also have short duration of action compared to drug-eluting implants.

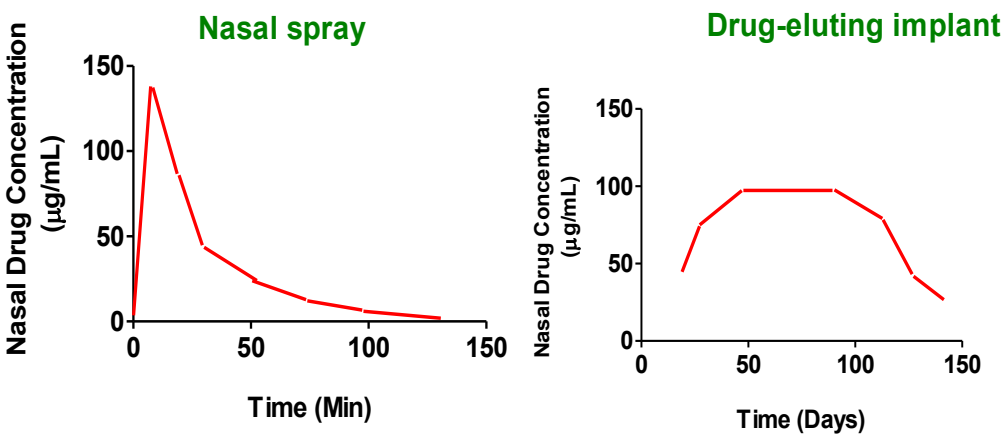

Figure 2 Comparison of the plots of nasal drug concentration versus time, obtained after administration of nasal sprays and drug-eluting implants.

1.4. Development of implants and the need for biodegradable/bioabsorbable impants

Most of the knowledge that is currently applied to nasal implants development was based on data acquired from cardiac stents. Bare metal stents (non-drug eluting) were the first of the approved stents, but are rarely used owing to the complications arising from their use. Metallic stents are known to cause stent thrombosis that requires prolonged antiplatelet therapy. Due to their rigid structure, lumen expansion is not possible[29,30]. Metallic stent backbone of drug-eluting stents can be coated with a polymer that serves as a vehicle for the drug and releases it in a controlled manner to the surrounding affected areas[30,31]. Even though drug-eluting metal stents significantly reduce the rate of restenosis, there are certain limitations associated with these stents. Late stent thrombosis and chronic inflammation at the stent site often occur[30,32]. Advances in stents research have led to the development of biodegradable stents and implants. These biodegradable drug-eluting devices are preferred over metal stents

because the late stent thrombosis does not occur with these materials. Biodegradable implants are made up of biodegradable polymeric materials that degrade *in vivo* over a prolonged period of time. The major advantage of these implants is that no additional surgeries are required to remove them[30].

1.5. Formulation considerations, biodegradable materials and drug candidates for formulating nasal drug-eluting stents

In chronic nasal conditions such as CRS, infection and inflammation become persistent and last for a very long time (>12 weeks)[18]. Therefore, sometimes it is necessary to achieve a sustained drug release over a long period of time (>2 months). This can be achieved by drug encapsulation in a biodegradable polymer matrix in form of micro or nano particles[33]. These micro or nano particles can then be incorporated in a biodegradable hydrogel to form a biodegradable implant[34]. The hydrogel degrades in a controlled fashion to release the drug-loaded microparticles, which in turn degrades slowly and consistently over a period of time to release the loaded drug. Ideally, biodegradable implants should release loaded drugs over a period of 2 to 6 months. Biodegradable polymers such as polylactic acid (PLA)[35,36] or polylactic-co-glycolic acid (PLGA)[37] can be used effectively for nasal implants as these materials have a long history of safety and effectiveness in humans[38]. PLA and PLGA are also used extensively for a variety of pharmaceutical applications, drug delivery devices and scaffolds fabrication for tissue engineering[39]. Other biodegradable polymers that can be used for nasal implants fabrication include complex sugars such as alginates[40], hyaluronates[41,42] and chitosan[43]. As for drug candidates for nasal stents, the most commonly used drugs for nasal

conditions include, but are not limited to: corticosteroids such as dexamethasone, fluticasone and mometasone, as well as antibiotics such as tobramycin and mupirocin[44].

1.6. Clinical applications of drug-eluting nasal implants

Incorporation of a drug such as corticosteroids, antibiotics or anti-neoplastic agents into nasal implants is the primary focus of developing drug-eluting nasal implants[45]. CRS is the primary medical indication for drug-eluting nasal implants. As nasal obstruction is the most common symptom of CRS[46], the aim of its treatment is to restore sinus ventilation, promote mucous drainage and reduce edema[12,47]. Although the first line of treatment for a patient with CRS is conservative medical therapy using antibiotics and corticosteroids, some patients with medically refractory CRS require functional endoscopic sinus surgery[7,12]. However, synechiae/adhesions and post-operative stenosis are the most common and troublesome complications following FESS[45,48]. Nasal implants can be used clinically as adjuncts to endoscopic sinus surgery to control hemorrhage, adhesions formation[49] and promote drainage of the sinus mucosa, thereby promoting wound healing[50]. Drug-eluting nasal implants have been reported to reduce the rate of synechiae and stenosis formation. As inflammation/polyp recurrence, adhesions, and middle turbinate lateralization following FESS are common outcomes; drug-eluting sinus implants can be used very effectively as adjuncts to sinus surgery because of their ability to preserve sinus patency by providing controlled and consistent drug release over a sustained period of time to the sinus mucosa[51].

1.7. Drug delivery applications of FDA-approved middle meatus implants

The middle meatus can be implanted with a spacer, implant or a sponge that preferably remains in place and is biodegradable releasing drug load (corticosteroid or antibiotic) over an extended period of time without causing any tissue damage[45]. Drug-eluting nasal implants not only improve the coverage of nasal passages, but also keep the middle meatus open following FESS[52,53]. The implants fill the ethmoid sinus cavity, which would otherwise be filled with blood and mucus[45]. Examples of clinically approved middle meatal implants include Propel™ implant[54], Relieva Stratus™ MicroFlow spacer[55] and the Sinu-Foam™ spacer[56,57].

1.7.1. Propel™ sinus implant

Recently in 2011, Propel™ sinus implant was approved by the US Food and Drugs Administration (FDA) to be used clinically for the treatment of CRS. It is a mometasone-eluting biodegradable implant that continuously releases the drug locally in a controlled manner and for a prolonged period of time[54]. Propel™ is a spring like device placed in the ethmoid sinus cavity (Figure 3) by the physician as an adjunct to FESS to prevent postoperative obstruction of the cavity, which can occur due to inflammation and scarring[54]. The drug-eluting material in Propel™ is biodegradable (PLGA). If this implant is placed in the affected sinus cavity, it is dissolved (biodegrades) releasing the potent corticosteroid (mometasone), which is embedded in the PLGA matrix. Propel™ implant has initiated a new era in the area of topical drug delivery for targeting the

affected sinus mucosa and providing controlled drug delivery directly to the sinus tissue[54]. However, presently propel implant is approved for use only in the USA[54].

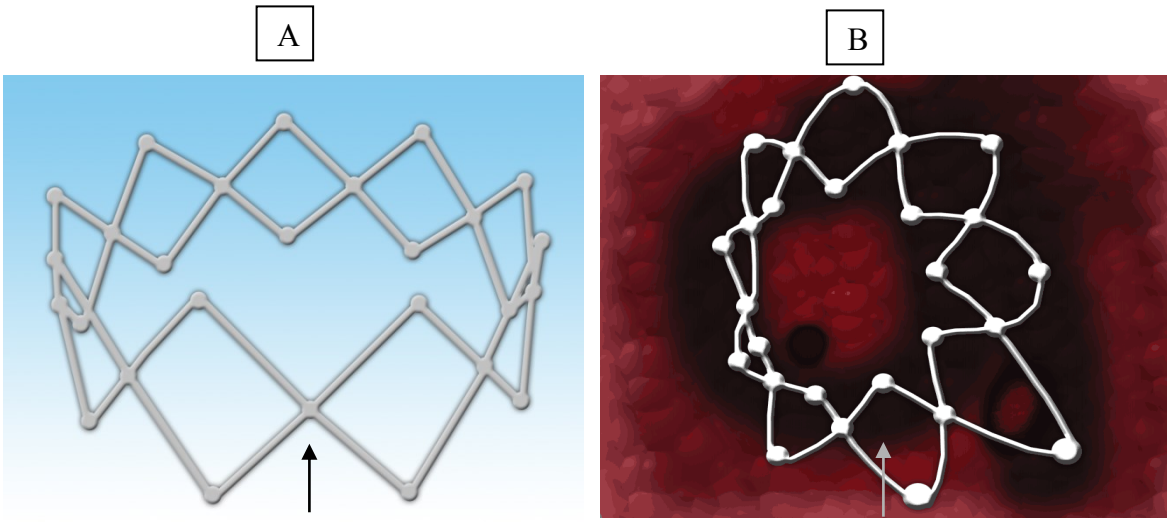

Figure 3 Mometasone-loaded spring-like Propel™ sinus implant (A) expands when placed into the sinus mucosa (B).

1.7.2. Relieva stratus™ microflow spacer

Acclarent (Menlo Park, CA, USA) introduced Relieva Stratus™ for the treatment of sinusitis[58]. Relieva Stratus™ is a drug-eluting nasal implant for the treatment of chronic ethmoid sinus mucosal disease. This device has two main components: the deployment guide and MicroFlow™ spacer. The design and components of Relieva Stratus™ Microflow spacer are shown in Figure 4 (deployment guide not shown). Basically, the MicroFlow spacer is a membrane reservoir surrounding a catheter shaft. The reservoir has several micropores that allow slow release of the instilled therapeutic agent into the target area. The device elutes the therapeutic agent slowly, continuously and in a controlled-manner for prolonged period of time. Relieva stratus™ is described as a minimally invasive option for the treatment of chronic ethmoid mucosal disease. It has

been demonstrated that the device emits the steroid triamcinolone acetate for about 2–4 weeks after which it is readily removed in a medical office setting[55,58]. Certain disadvantages are associated with this device. It has been considered to be a leaky balloon instead of a conventional implant because of its fast drug release[59]. This device is temporary, requiring manual removal after 30 days and a new device may be implanted, if needed[60]. This device also is not suitable for patients with extensive polyps[55]. Finally, certain adverse events have been reported for the device[58] and orbital violation following its placement has been reported[61]. Although Relieva stratus™ can potentially be used with any therapeutic agent, it is currently approved by the FDA for use only with saline. This device is not intended for use with active drug substances as the safety and effectiveness of the device has not been demonstrated with an active drug substance in the reservoir. Use of steroids might result in high local and/or systemic concentrations, which may lead to serious adverse events[62]. Relieva stratus™ is no longer marketed in the United States[60].

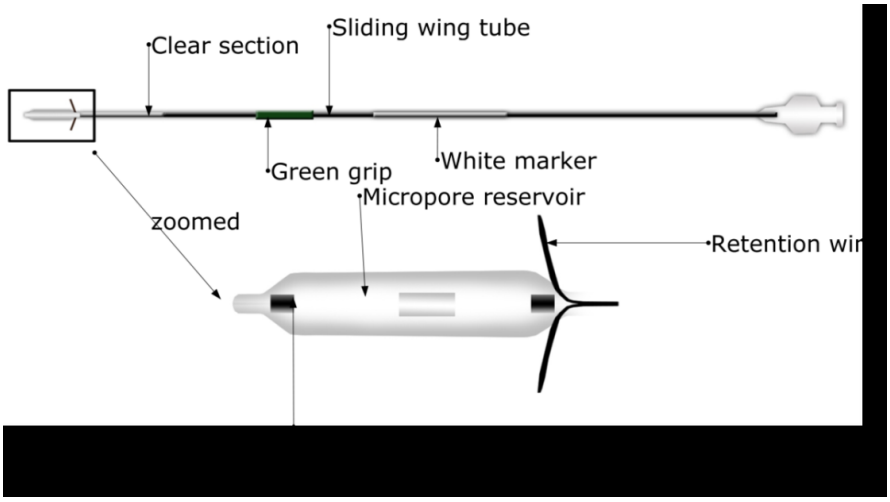

Figure 4 A typical design of a Relieva Stratus™ Microflow spacer, which contains a microporous reservoir.

1.7.3. Sinu-Foam™ spacer

Sinu-Foam™ is an FDA-approved mixture, which is commonly mixed with saline and gently placed in the ethmoid cavity following FESS[56]. A dexamethasone Sinu-Foam™ spacer was evaluated following FESS for CRS without polyps[57]. The spacer was found to promote wound healing of the nasal and sinus mucosa by reducing the inflammation associated with CRS[56]. However, its clinical utility remains a debate since it does not improve endoscopic outcomes in the early postoperative period following FESS[57]. It is not yet approved for use with steroids.

Currently Propel™ is the only FDA approved implant on the market which shows sustained release of mometasone for a duration of 30 days. Thus, a sustained release drug delivery system capable of releasing the drug for a prolonged period of time (2 to 6 months) can be potentially used for CRS, which lasts for a duration of 12 weeks.

CHAPTER 2 OBJECTIVES AND SCOPE

The aim of the study was to develop a sustained release biodegradable drug delivery system, which is expected to release entrapped drug locally to the affected sinus mucosa slowly and continuously for about 2-6 months. As CRS is a condition which has a severe impact on the patient's quality of life and lasts for a period longer than 12 weeks, it is important to develop a biodegradable drug delivery system that delivers loaded drug over a prolonged period of time.

To accomplish this, our research objectives were as follows:

a. To develop and characterize dexamethasone-loaded PLGA microparticles
b. To incorporate the microparticles loaded with dexamethasone into a chitosan sponge implant delivery system.
c. To incorporate the drug-loaded microparticles into alginate hydrogel implant delivery system.
d. To use PLGA microparticles loaded with rhodamine 6G, a hydrophobic dye with a molecular weight comparable to dexamethasone, our model compound to determine the extent and possible mechanisms of uptake of PLGA microparticles by respiratory epithelial cells.

CHAPTER 3 MATERIALS AND METHODS

3.1. Chemicals

Poly(D,L-lactide-co-glycolide) (PLGA, lactide:glycolide 50:50, MW 54000 to 69000), PLGA (lactide:glycolide 50:50, MW 24000 to 38000), PLGA (lactide:glycolide 65:35, MW 24000 to 38000), polyvinyl alcohol, (PVA, MW 13000-23000, 87-89% hydrolyzed), PVA (MW 31000-50000, 98-99% hydrolyzed), dichloromethane (DCM), sodium bicarbonate, guanosine 5'-diphosphate sodium salt (GDP) and sodium alginate were purchased from Sigma-Aldrich (Oakville, ON, Canada). High Performance Liquid Chromatography (HPLC) grade dexamethasone, calcium chloride anhydrous and rhodamine 6G dye were purchased from Santa Cruz Biotechnology Inc. (Dallas, TX, USA). HPLC grade acetonitrile (ACN), amyl acetate and dimethylsulfoxide (DMSO) were purchased from Fischer Scientific (Ottawa, ON, Canada). HPLC grade methanol was purchased from EMD Millipore (Billerica, MA, USA). High molecular weight chitosan (degree of deacetylation > 90%; 3000 cp viscosity) was procurred from MP Biomedicals (Solon, OH, USA). Rhodamine 6G-loaded PLGA microparticles (0.2 to 0.3 μm) were supplied by Phosphorex Inc. (Hopkinton, MA, USA).

3.2. Cell culture media and other components

Fetal bovine serum (FBS), GlutaMAX®, penicillin-streptomycin, DMEM F-12 and TRIzol® were purchased from Life technologies Inc. (Burlington, ON, Canada). Phosphate Buffered Saline (PBS, 10X) and Hanks Balanced Salts Solution (HBSS), with and without $Ca^{2+}$and Mg^{2+} were purchased from Sigma-Aldrich (Oakville, ON, Canada). Ultracruz® 24 well tissue culture plates were purchased from Santa Cruz Biotechnology Inc. (Dallas, TX, USA). HEPES was purchased from Fisher Scientific (Ottawa, ON, Canada).

3.3. Analytical method optimization and validation

Calibration curves and stock solutions for dexamethasone were prepared using the method described in the United States Pharmacopoeia (USP). A stock solution of 0.3 mg/ml was used. To prepare the stock solution, 1 mg of dexamethasone was dissolved in 1 ml of methanol to give 1 mg/ml solution. A 0.3 ml aliquot of this solution was diluted to 1 ml with mobile phase (acetonitrile: water 60:40) to give the final stock solution of 0.3 mg/ml. Standard dexamethasone concentrations of 0.1, 0.5, 1, 10 and 100 µg/ml were prepared from the stock solution. Runs were conducted with C18 reverse phase column (3.9 x 150 mm^2) set at 35 °C and a flow rate of 1 ml/min. The HPLC method used to quantify dexamethasone was validated according to the International Conference on Harmonization (ICH) Guidelines as described below[63].

3.3.1. HPLC method validation: Limit of quantification (LOQ), range and linearity

LOQ is the lowest concentration of the analyte which can be quantified with acceptable accuracy and precision. LOQ is the lower limit of the range; whereas the upper limit of the range is determined based on the expected drug concentrations in the samples and the highest concentration at which acceptable accuracy and precision is obtained. Standard calibration curves were obtained using five standard concentrations over a range of 0.1 to 100 μg/ml (0.1, 0.5, 1, 10 and 100 μg/ml). Peak area (AUC) was plotted against drug concentration and a standard equation was obtained.

3.3.2. HPLC method validation: Accuracy

For determination of HPLC method accuracy, three quality control (QC) standard samples (1.5 μg/ml, 15 μg/ml and 50 μg/ml) were injected into the HPLC in triplicates and percentage recovery was determined.

3.3.3. HPLC method validation: Precision

As per the ICH guidelines, precision of the method was determined by analyzing the QC standards at three concentrations (low QC = 0.75 μg/ml, Intermediate QC = 5 μg/ml and High QC = 60 μg/ml). The method was checked for repeatability (intra-day precision) and reproducibility (inter-day precision). For intra-day precision, the QC standard samples were injected into the HPLC in triplicates on the same day and percentage co-efficient of variation (% CV) of analyte peak was determined. For inter-day precision, the three QC standard samples were injected in triplicates on three different days and percentage CV was determined.

3.4. Preparation of microparticles

Biodegradable blank microspheres (without the drug) and drug-loaded (dexamethasone) microparticles were prepared using oil-in-water (O/W) emulsion-solvent evaporation method. For blank microparticles, 50 mg of PLGA was dissolved in 1.5 - 3.75 ml of a volatile organic solvent, dichloromethane (DCM) or 0.75 - 3 ml of DCM: Methanol (5:1) mixture to give the organic phase. Aqueous phase consisted of 10 - 62.5 ml of 0.2 % w/v or 0.3 % w/v PVA (MW 13000-23000, 87-89% hydrolyzed) solution or 62.5 ml of 2% w/v PVA (MW 31000-50000, 98-99% hydrolyzed) solution as an emulsifier. For drug-loaded microparticles, 10 mg of dexamethasone was added to the organic phase (PLGA solution). When preparing the microparticles, organic phase was added to the aqueous phase drop wise using a 1 ml syringe, with simultaneous stirring at 10,000 rpm (using a high speed homogenizer FJ200 USG) which resulted in O/W emulsion. This emulsion was stirred on a magnetic plate at 100 rpm for 18 hours to evaporate the organic solvent. The microparticles were collected by centrifugation at 3,000 rpm (using Eppendorf Centrifuge 5810 R). The microparticles were then washed four times with double distilled de-ionized water and were frozen overnight at -20 °C using 25% sucrose as a cryoprotectant. The frozen microparticle suspension was then lyophilized for 24 hours and the dried microparticulate powder was stored at -20 °C till further use. Several microparticle formulations were developed with different combinations and ratios of the organic and aqueous phase solvents, different concentrations of PVA and different grades of PLGA and PVA (Table 1 and Table 2) and the best suitable formulations were optimized.

Table 1 Conditions for the development of various microparticle formulations.

Formulation codes	PLGA	Organic phase	Emulsifier	Aqueous Phase
F-1	50:50, 54k-69k	DCM 2 ml	PVA 87-89% hydrolyzed	20 ml of 0.3% PVA
F-2	50:50, 54k-69k	DCM : Methanol (5 : 1) 3 ml	PVA 87-89% hydrolyzed	20 ml of 0.3% PVA
F-3	50:50, 54k-69k	DCM 3.75 ml	PVA 87-89% hydrolyzed	62.5 ml of 0.2% PVA
F-4	50:50, 24k-38k	DCM 3.75 ml	PVA 87-89% hydrolyzed	62.5 ml of 0.2% PVA
F-5	50:50, 54k-69k	DCM 3.75 ml	PVA 98-99% hydrolyzed	62.5 ml of 2% PVA
F-6	65:35, 24k-38k	DCM 3.75 ml	PVA 98-99% hydrolyzed	62.5 ml of 2% PVA

Table 2 Conditions for the development of new microparticle formulations based on formulations F-1 to F-6.

Formulation codes	PLGA	Organic phase	Emulsifier	Aqueous Phase
F-1'	50:50, 54k-69k	DCM 1.5 ml	PVA 87-89% hydrolyzed	10 ml of 0.3% PVA
F-2'	50:50, 54k-69k	DCM : Methanol (5 : 1) 0.75 ml	PVA 87-89% hydrolyzed	10 ml of 0.3% PVA
F-3'	50:50, 54k-69k	DCM 1.5 ml	PVA 87-89% hydrolyzed	20 ml of 0.2% PVA
F-4'	50:50, 24k-38k	DCM 1.5 ml	PVA 87-89% hydrolyzed	20 ml of 0.2% PVA
F-5'	50:50, 54k-69k	DCM 1.5 ml	PVA 98-99% hydrolyzed	20 ml of 2% PVA
F-6'	65:35, 24k-38k	DCM 1.5 ml	PVA 98-99% hydrolyzed	20 ml of 2% PVA
F-7	50:50, 54k-69k	DCM 1.5ml	PVA 87-89% hydrolyzed	20 ml of 0.3% PVA
F-8	50:50, 54k-69k	DCM : Methanol (5 : 1) 0.75 ml	PVA 87-89% hydrolyzed	20 ml of 0.3% PVA

These formulations were made by modifying the volumes of the organic and aqueous phases.

3.5. Characterization of microparticles

To optimize the formulations, the microparticles were monitored for PLGA degradation, particle morphological appearance, size distribution, mean particle size, loading efficiency, encapsulation efficiency and *in vitro* drug release. These studies were performed using freeze-dried samples.

3.5.1. PLGA degradation studies

An aliquot (10 mg) drug-free (blank) microparticles were suspended in 10 ml PBS (pH 7.4) containing 0.1% w/w sodium azide and 2% v/v Tween 80. The suspension was placed on a shaker regulated at 37°C. At pre-determined time intervals (every 24 hours for one week; and once a week thereafter for 15 weeks), the pH of the suspension was recorded and a plot of pH vs time was obtained[64].

3.5.2. Mean particle size and size distribution of microparticles

In these studies, the microparticles (1 mg/ml) were suspended in PBS, pH 7.4. The microparticles suspension was injected in to the Micro-Flow Imaging (Brightwell technologies DPA 4100) using a 1 ml micropipette. The suspension was then allowed to pass through a flow-cell with size range from 2.5 - 100 μm (capable of detecting particles as low as 0.75 μm). The microparticles images were observed. The mean particle sizes and size distribution profiles were also determined.

3.5.3. Determination of loading and encapsulation efficiency of the microparticles

For these studies, 2 mg of dexamethasone-loaded microparticles was dissolved in 2 ml DMSO: acetonitrile: water (2: 4.8: 3.2) to give 1 mg/ml of microparticle solution. This solution was then injected into the Varian 920-LC chromatography unit (Agilent Technologies, Mississauga ON, Canada). Dexamethasone peak area was determined and the drug content (mg) in the microparticles was then analyzed using the dexamethasone standard curve equation.

The loading efficiency (%) was determined using the following equation[65]:

Loading efficiency = (mg of dexamethasone / mg of microspheres) X 100

Also, the encapsulation efficiency (%) was determined as follows**Error! Bookmark not defined.**:

Encapsulation efficiency = (Experimental drug loading / Theoretical drug loading) X 100

3.5.4. *In vitro* dexamethasone release profile from microparticles

The release medium comprised of PBS (pH 7.4) supplemented with 0.1% w/v sodium azide and 2% v/v Tween 80 to prevent microparticles contamination and agglomeration, respectively[66,67]. 10 mg of microparticles was suspended in 5 ml of the release medium in 15 ml centrifuge tubes. The suspension was placed on a shaker maintained at 37°C. At pre-determined time intervals (every 24 hours for one week; and once a week thereafter for 13 weeks), the tubes were centrifuged and 1 ml of the supernatant was withdrawn for HPLC analysis and the tubes were replenished with 1 ml

of fresh release medium to maintain a sink condition. Plot of percent cumulative dexamethasone release vs. time was obtained.

3.5.5. Morphological studies

The surface morphology of the microparticles was observed using Scanning Electron Microscope (SEM) (ZEISS-1455VP). Freeze-dried microparticles were sprinkled on aluminum stubs and were observed under SEM after gold-palladium spluttering using Leica EM ACE200.

Surface morphology, cross-linking intensity and porosity of the alginate and chitosan sponges was observed using Scanning Electron Microscope (SEM) (ZEISS-1455VP). Dried sponges were crushed and mounted on aluminum stubs and viewed under SEM after gold-palladium spluttering using Leica EM ACE200.

3.5.6. X-ray diffraction studies

X-ray diffraction (XRD) studies were performed using D8 advance high speed XRD system (Bruker, Milton, ON). Samples for XRD were dexamethasone, PLGA (50:50, 54k-69k), blank PLGA microparticles, dexamethasone-loaded microparticles F-7 and F-8, rhodamine 6G and rhodamine 6G-loaded microparticles. Dried powders were placed in the sample holder and exposed to a graphite monochromatized copper radiation (wavelength= 1.5406 nm, 40kV, 40 mA). Samples were measured in the 2 theta (2θ) range from 5° to 60° at a scanning rate of 3°/min.

3.6. Preparation of calcium alginate sponges

Microparticles developed and optimized using the methods described above were incorporated into calcium alginate sponge network. Calcium alginate sponges were prepared using ionic cross-linking process[40]. Dexamethasone-loaded microparticles were suspended in aqueous sodium alginate solution (1 or 2%), which was cross-linked with aqueous calcium chloride solution (1%). Calcium alginate hydrogels obtained were subsequently dried using a critical point dryer (Leica CPD 300).

3.7. Characterization of calcium alginate sponges

3.7.1. Entrapment efficiency of alginate sponges

Entrapment efficiency of the sponges was determined by an indirect method. Calcium chloride solution when added to the sodium alginate solution forms a hydrogel, which on drying develops the highly cross-linked sponge, which is difficult to dissolve in a solvent for determination of entrapment efficiency. Thus, the remaining supernatant after formation of the hydrogel was analyzed for dexamethasone content. This gave the non-entrapped amount of dexamethasone microparticles. This, when subtracted from the theoretical amount of microparticles used for the development of the sponges gave the actual amount of microparticles entrapped in the calcium alginate sponges.

3.8. Preparation of chitosan sponges

Chitosan based sponges were also developed as a drug delivery system for the microparticles[68]. To develop a sustained release implant, dexamethasone-loaded microparticles were incorporated into chitosan sponge network. For preaparation of the chitosan sponges, 10 ml of 0.06 M HCl solution was added to each of the 4 beakers. In two of the beakers, 30 mg of chitosan was added (3 mg/ml) and in the remaining two beakers, 60 mg of chitosan was added (6 mg/ml) and stirred for 30 min to completely dissolve the chitosan. The pH of the 3 mg/ml chitosan solution was adjusted to 5 $\pm$ 0.05 (labelled as C3PH5) and the pH of other 3 mg/ml chitosan solution was adjusted to 6 $\pm$ 0.05 (labelled as C3PH6). Similarly, two beakers containing 6 mg/ml chitosan solutions were adjusted to pH 5 and pH 6 to give C6PH5 and C6PH6, respectively. Then, 1.7 ml of each of the 4 chitosan solutions (C3PH5, C3PH6, C6PH5, and C6PH6) were added to Eppendorff tubes and followed by 2 mg of dexamethasone-loaded microparticles.. Furthermore, 150 mg of GDP was dissolved in 1.5 ml of water (100 mg/ml) and 0.3 ml of the GDP solution was rapidly added to each of the 4 chitosan solutions (in Eppendorff tubes containing suspended microparticles). This resulted in thick chitosan sponges that were subsequently dried using a critical point dryer (Leica CPD 300).

3.9. *In vitro* cellular uptake studies

Rhodamine 6G is a hydrophobic dye and has a molecular weight of 479.1 g/mol. Dexamethasone is also a hydrophobic corticosteroid with a molecular weight of 392.5 g/mol. In terms of hydrophobicity and molecular weght, rhodamine 6G is comparable to dexamethasone. The purpose of these studies was to determine whether respiratory epithelial cells were capable of taking up microparticles of comparable sizes to our formulations. The type of PLGA for rhodamine microparticles was the same as dexamethasone microparticles. Intracellular accumulation of rhodamine 6G was analyzed using a Modulus^{TM} single tube multimode reader fluorometer (Turner BioSystems, Madison, United States).

3.9.1. Effect of incubation time on the uptake of rhodamine 6G dye and rhodamine 6G microparticles

Calu-3 and nasal cell monolayers were incubated with 2 μM of rhodamine 6G dye at 37°C for 0 to 4 h (0, 15, 30, 60 and 120 min). Similarly, Calu-3 and nasal cell monolayers were exposed to 100 μg/ml of rhodamine 6G microparticles. Cells were incubated at 37°C for 0 to 4 hrs (0, 15, 30, 60 and 120 min). After the desired incubation time, cells were dissolved in 1% Triton-X 100 solution with 0.1N sodium hydroxide and analyzed with fluorometer. All studies were conducted in triplicates. Protein assay was also performed for each well according to manufacturer's protocol. A plot of uptake (μg/mg protein/cm^2) vs time was obtained.

3.9.2. Effect of concentration on the uptake of rhodamine 6G dye and rhodamine 6G microparticles

Calu-3 and nasal cell monolayers were incubated at 37°C with concentrations of 1, 2, 5, 10 and 20 µM of rhodamine 6G dye for 30 min. Similarly, Calu-3 and nasal cell monolayers were incubated at 37°C with concentrations of 100, 200, 500 and 1000 µg/ml of rhodamine 6G microparticles for 30 min. All studies were performed in triplicates. After the desired incubation time (30 min), cells were treated and analyzed as described in section 3.9.1. A plot of uptake (µg/mg protein/cm^2) vs time was obtained.

3.9.3. Effect of incubation temperature on the uptake of rhodamine 6G dye and rhodamine 6G microparticles

Calu-3 and nasal cell monolayers were incubated with 2 µM of rhodamine 6G dye for 30 min at 37°C and 4°C. Similarly, Calu-3 and nasal cell monolayers were incubated with 100 µg/ml of rhodamine 6G microparticles for 30 min at 37°C and 4°C. All studies were performed in triplicates. After the desired incubation time (30 min), cells were treated and analyzed as described in section 3.9.1. A plot of uptake (µg/mg protein/cm^2) vs time was obtained.

3.9.4. Effect of pH on the uptake of rhodamine 6G dye and rhodamine 6G microparticles

Calu-3 and nasal cell monolayers were incubated at 37°C with 2 µM of rhodamine 6G dye for 30 min at pH 5.5 (acidic), pH 7.4 (physiological) and pH 8.5 (alkaline). Similarly, Calu-3 and nasal cell monolayers were incubated at 37°C with 100 µg/ml of rhodamine 6G microparticles for 30 min at pH 5.5 (acidic), pH 7.4

(physiological) and pH 8.5 (alkaline). All studies were performed in triplicates. After the desired incubation time (30 min), cells were treated and analyzed as described in section 3.9.1. A plot of uptake (μg/mg protein/cm^2) vs time was obtained.

4. Statistical data analysis

For all *in vitro* uptake experiments, student t-test was used to determine the statistical differences (P value) between the uptake of free rhodamine 6G dye and rhodamine 6G-loaded microparticles.

CHAPTER 4 RESULTS

4.1. Analytical method development and optimization

Dexamethasone was analyzed and quantified using HPLC. The mobile phase used was acetonitrile: water (60:40) with column temperature set at 35°C. The HPLC chromatogram obtained after injection of 100 µg/ml, 50 µg/ml and 10 µg/ml of dexamethasone (Figure 5) shows a retention time of 1.40 min. Run time was 3 min.

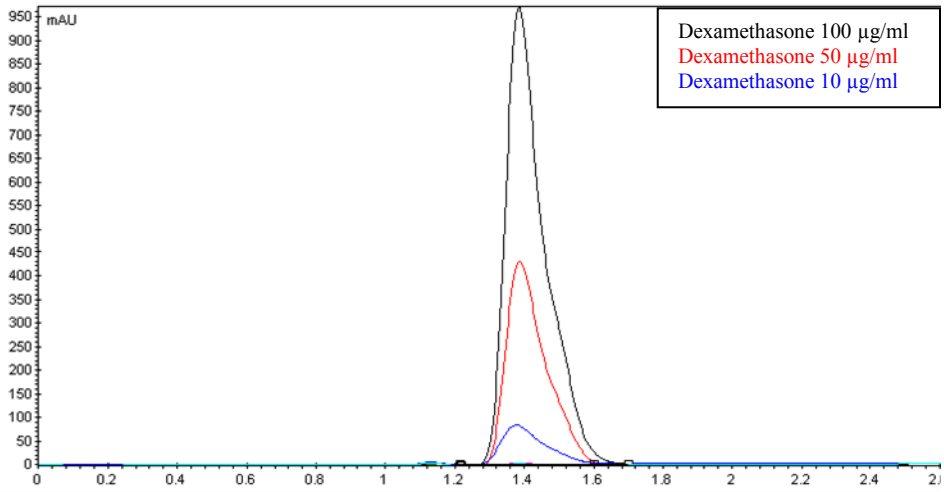

Figure 5 HPLC chromatogram for 100 µg/ml, 50 µg/ml and 10 µg/ml dexamethasone.

4.1.1. Linearity

Linearity of the HPLC method was confirmed using five dexamethasone standard concentrations in the analytical range of 0.1-100 µg/ml (0.1, 0.5, 1, 10 and 100 µg/ml). A standard curve representing this range is shown in Figure 6. A linear regression between the analyte peak areas and the amount injected into the HPLC was observed. The co-efficient of determination (R^2) was 1.00 and the standard equation was y = 1.265x +

0.1753. Range was optimized based on the expected concentrations of dexamethasone in the samples during experiments.

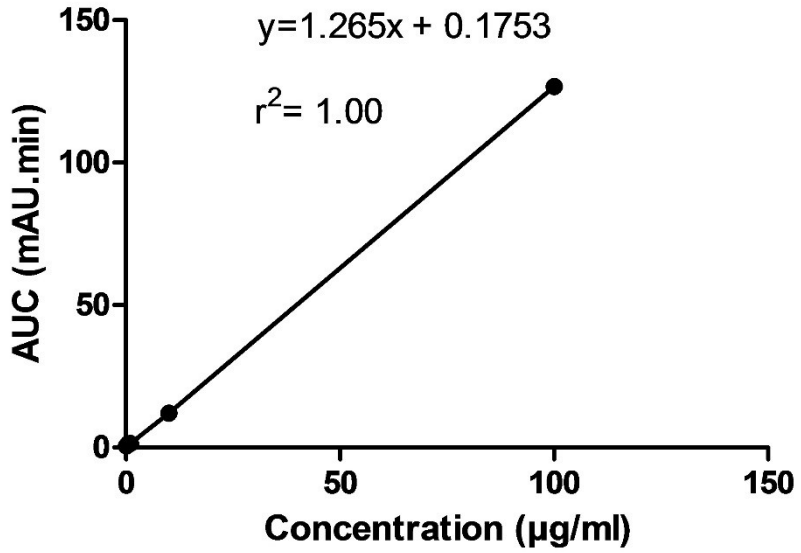

Figure 6 Linearity of dexamethasone within a concentration range of 0.1-100 µg/ml

4.1.2. Accuracy

Accuracy was established across the linear analytical range (0.1-100 µg/ml). Results for accuracy of the analytical method are summarized in Table 3. The table shows the percentage recovery, which were within the 95 % - 105 % acceptable range for early stages of formulation development activities.

Table 3 Accuracy of dexamethasone quantification with Varian 920 LC system

Nominal Concentration	1.5 µg/ml	15 µg/ml	50 µg/ml
Amount Recovered µg/ml	1.51	14.77	49.63
	1.52	14.74	49.57
	1.53	14.79	49.55
Mean	1.52	14.77	49.58
Standard Deviation	0.01	0.02	0.04
Percent RSD	0.66	0.17	0.08
Percent Recovery	101.33	98.47	99.16

4.1.3. Precision

In repeatability studies, three dexamethasone QC standards: low (0.75 µg/ml), intermediate (5 µg/ml) and high (60 µg/ml) were analyzed and their mean percent coefficients of variation for intra-day studies were 0.76 %, 0.19 % and 1.36 %, respectively. The mean percent coefficients of variation for inter-day studies were 3.1%, 0.70 % and 1.99 %. All the results obtained were within the acceptable limit of 5 %[69]. Repeatability (intra-day) and inter-day precision data are summarized in Table 4.

Table 4 Repeatability and interday precision for dexamethasone assay.

		Conc. (µg/ml)	Repeatability (intra-day)			Inter-day		
			Mean	SD	CV (%)	Mean	SD	CV (%)
Low QC standard 0.75 µg /ml	**Day 1**	0.77 0.78 0.77	0.77	0.006	0.78	0.79	0.025	3.1
	Day 2	0.79 0.80 0.79	0.79	0.006	0.76			
	Day 3	0.82 0.82 0.81	0.82	0.006	0.73			
Intermediate QC standard 5 µg/ml	**Day 1**	5.07 5.05 5.07	5.06	0.011	0.22	5.02	0.035	0.70
	Day 2	4.99 4.99 5.01	4.99	0.011	0.23			
	Day 3	5.02 5.02 5.01	5.02	0.006	0.12			
High QC standard 60 µg/ml	**Day 1**	62.60 62.93 63.79	63.11	0.614	0.97	61.89	1.235	1.99
	Day 2	59.41 61.01 61.50	60.64	1.093	1.80			
	Day 3	62.72 61.11 61.99	61.94	0.806	1.30			

4.2. Preparation of microparticle formulations

Different formulations were prepared using various grades and concentrations of the emulsifier (PVA), the polymer (PLGA) and different combinations of the organic / aqueous phase volumes. Initial microparticle formulations were prepared using the references available in literature[64,65,66]. However, some of the initial formulations were unstable and resulted in polymer precipitation. Thus, it was necessary to vary the emulsifier grade and concentrations, polymer (PLGA) grades, organic and aqueous phase volumes so as to develop stable microparticle emulsions. Thus, the conditions for development of stable emulsions were optimized. Microparticle formulations F-1 to F-6 (Table 1) were stable and appeared cloudy but no precipitation. These formulations appeared as tiny dots under Hund Wetzlar microscope (Fisher Scientific, Ottawa, Ontario). These formulations were then lyophilized to obtain dry microparticles that were further characterized. Based on the characterization results (discussed in subsequent sections), formulations F-1 to F-6 were further optimized to give formulations F-1' to F-6', F-7 and F-8 (Table 2).

4.3. Characterization and optimization of the microparticle formulations

4.3.1. PLGA degradation studies

PLGA degradation studies were carried out with blank microparticle formulations (F-1 to F-6) to determine how long it would take the PLGA matrix to break down. This was important as we intended to develop nasal implants expected to be biostable for 2 – 6

months. These studies were not performed for modified formulations F-1' to F-6', F-7 and F-8 as the type of PLGA is the same and the degradation profile for these formulations are expected to be the same as that of formulations F-1 to F-6. It was observed that the PLGA used for the formulations degraded very slowly over a period of more than 3 months (Figure 7). All the studies were performed in triplicates and the error bars (standard deviations) were too small to be observed in the graphs. PLGA degradation studies were of great significance as it enabled us to determine the slow degradation profiles of PLGA that was selected for the studies. Thus, drug-loaded PLGA microparticles were expected to release drug loads in a sustained manner following slow degradation of the PLGA.

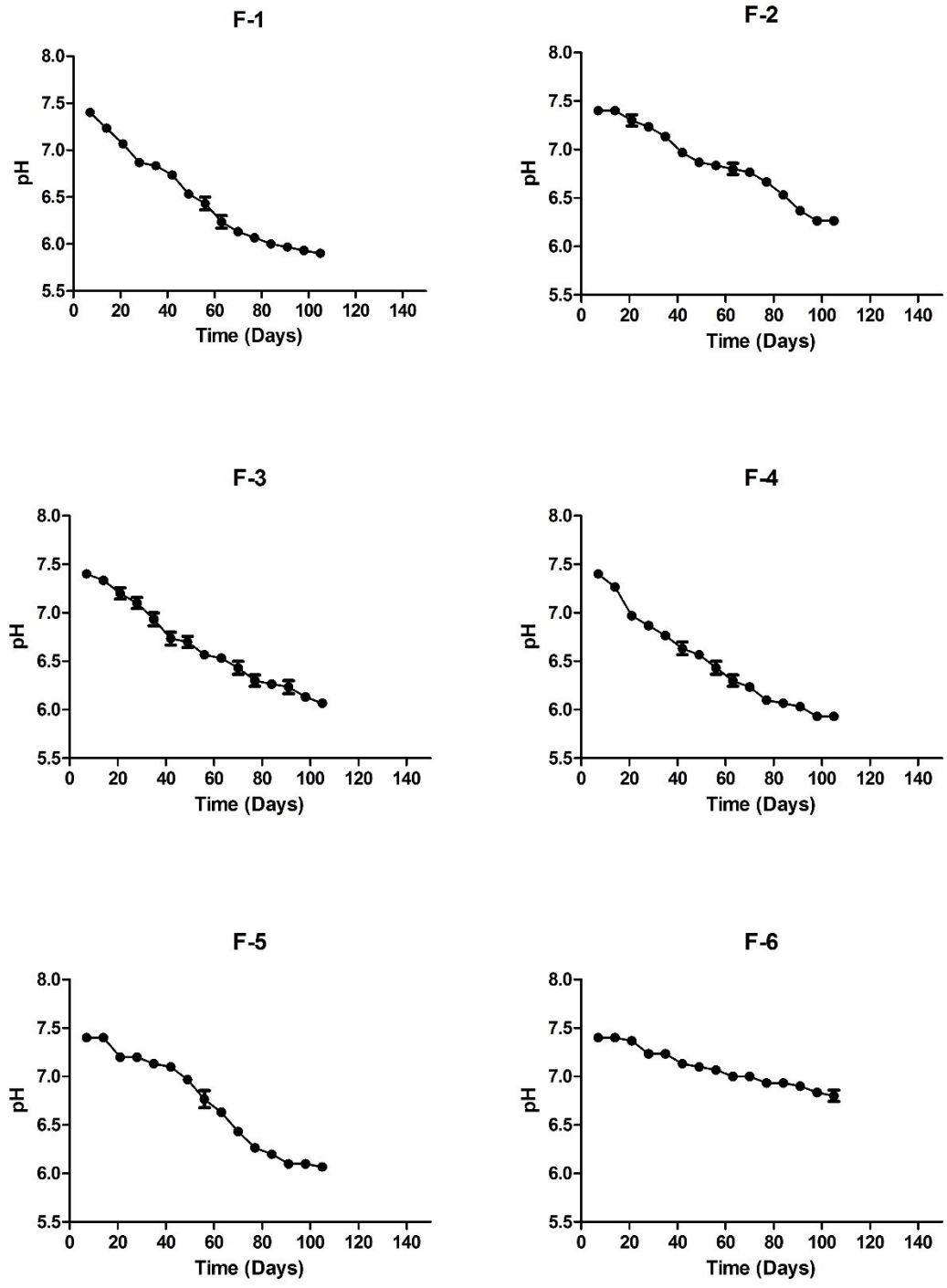

Figure 7 Degradation profiles of blank PLGA microparticle formulations (F-1 to F-6).

4.3.2. Mean particle size and size distribution studies

Mean particle size and size distribution of the microparticles was determined using Micro-Flow Imaging®. It can be observed in Table 5 that the mean particle size of all formulations is in the range of 1.50 to 2.00 μm.

Table 5 Mean particle sizes of dexamethasone-loaded microparticle formulations

Formulation codes	**Mean particle size (μm)**
F-1	1.74 ± 1.55
F-2	1.51 ± 1.30
F-3	1.76 ± 1.57
F-4	1.42 ± 1.52
F-5	1.73 ± 1.03
F-6	1.59 ± 1.08
F-7	1.85 ± 1.69
F-8	1.96 ± 1.43

Figure 8 shows the size distribution profiles and the images obtained with Micro-Flow Imaging system for formulations F-1 to F-6.

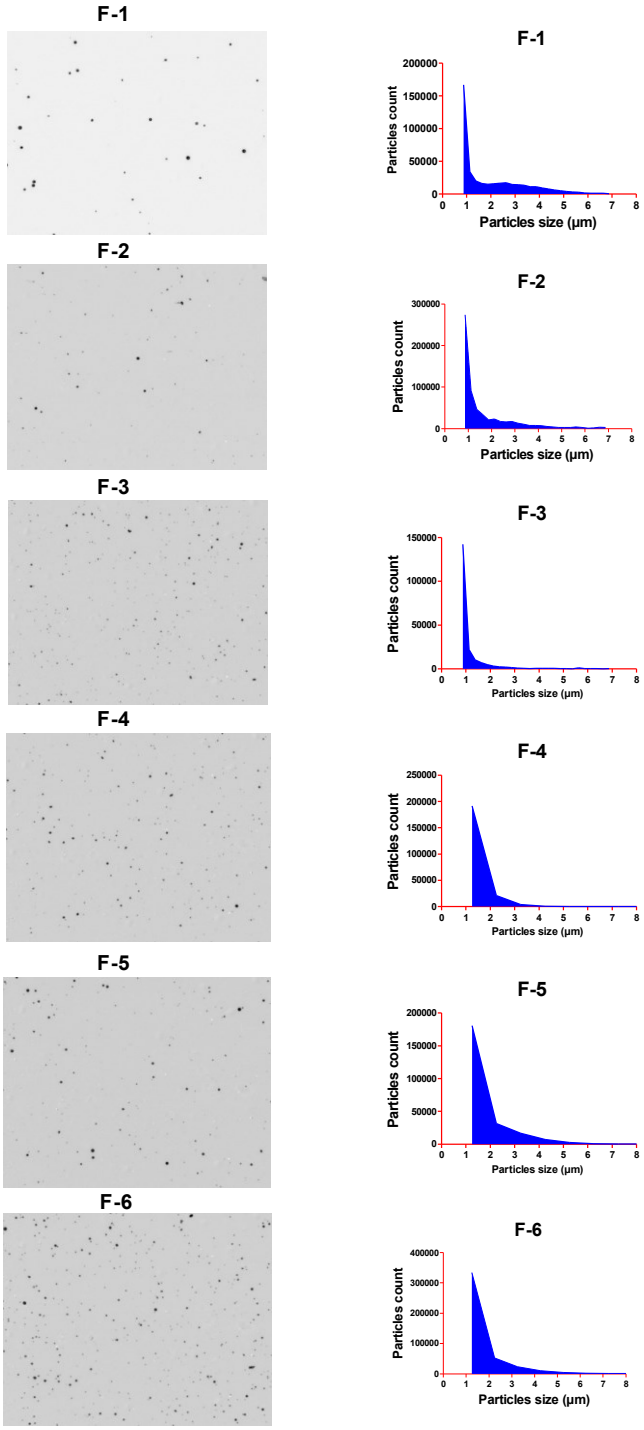

Figure 8 Microparticle images and particles size distribution (particles count vs particles size) of dexamethasone-loaded PLGA microparticles (F-1 to F-6).

Figure 9 shows the size distribution profiles and images for optimized formulations F-7 and F-8. The microparticles were observed as small dots and the size distribution for all the formulations were plotted as particles count vs particles size in µm. As Micro-Flow Imaging enabled visual observation of the microparticles, it was a useful preliminary indicator of the spherical shape of the microparticles.

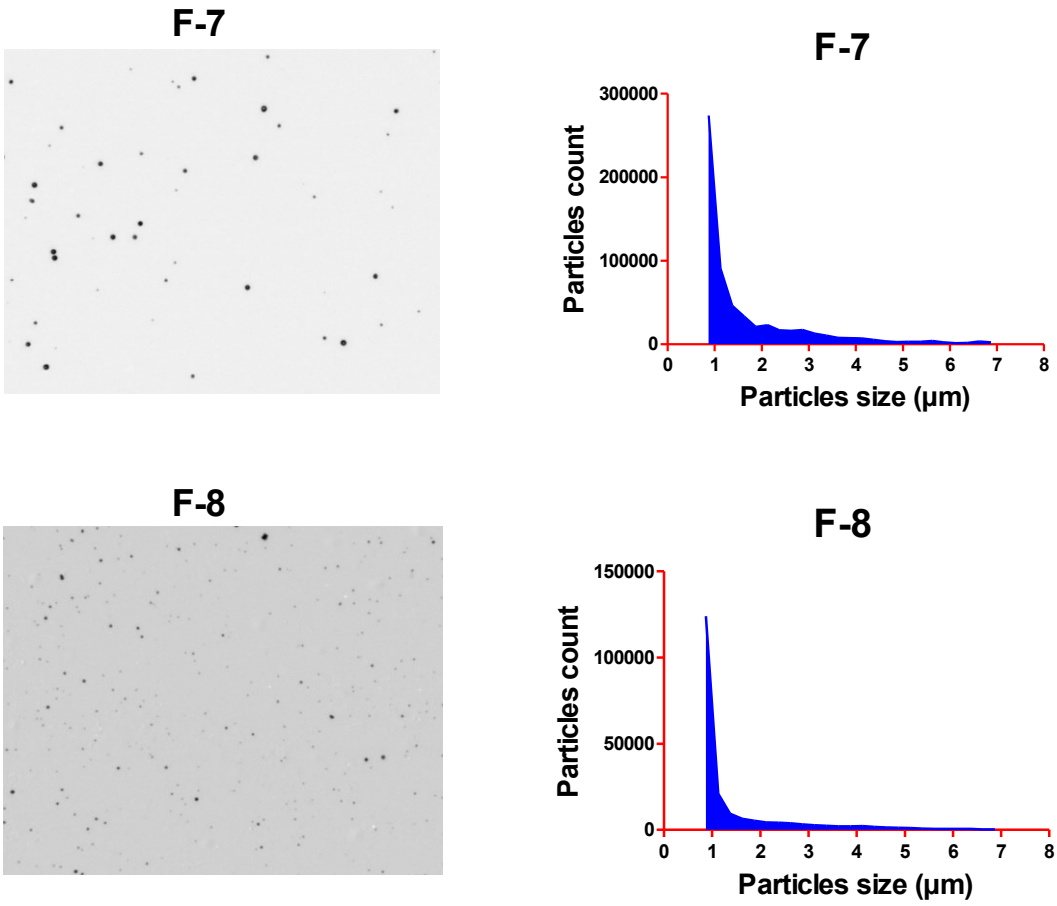

Figure 9 Microparticle images and particles size distribution (particles count vs particles size) of dexamethasone-loaded PLGA microparticles (F-7 and F-8).

4.3.3. Loading and encapsulation efficiency of microparticles

The encapsulation and loading efficiency (%) of dexamethasone-loaded microparticle formulations (F-1 to F-6) are shown in Table 6.

Table 6 Encapsulation and loading efficiency of microparticles formulations.

Formulation codes	**Encapsulation Efficiency (%)**	**Loading Efficiency (%)**
F-1	35.61 ± 0.88	7.12 ± 0.18
F-2	32.76 ± 1.13	6.55 ± 0.23
F-3	19.84 ± 1.25	3.97 ± 0.25
F-4	20.09 ± 1.71	4.01 ± 0.34
F-5	9.94 ± 1.75	1.99 ± 0.35
F-6	10.38 ± 1.19	2.08 ± 0.24

It was observed that the encapsulation and loading efficiency of formulations F-1 to F-6 were low. Thus, these formulations were modified by altering the organic and aqueous phase volumes. The conditions for developing improved formulations (F-1' to F-6', F-7 and F-8) are shown in Table 2 (Materials and Methods section). The encapsulation and loading efficiency for the modified formulations were evaluated and the results are shown in Table 7.

Table 7 Encapsulation and loading efficiency of improved microparticle formulations.

Formulation codes	Encapsulation Efficiency (%)	Loading Efficiency (%)
F-1'	35.70 ± 0.66	7.14 ± 0.13
F-2'	31.51 ± 1.37	6.29 ± 0.27
F-3'	13.89 ± 1.89	2.78 ± 0.38
F-4'	15.92 ± 1.32	3.18 ± 0.26
F-5'	22.82 ± 2.79	4.56 ± 0.56
F-6'	23.54 ± 1.04	4.71 ± 0.21
F-7	41.00 ± 1.45	8.20 ± 0.29
F-8	54.47 ± 1.63	10.89 ± 0.33

It was observed that the encapsulation and loading efficiency of the modified formulations (F-1', F-2', F-3' and F-4') were similar to formulations F-1, F-2, F-3 and F-4, respectively. However, the encapsulation efficiency of modified formulations F-5' and F-6' were approximately 2.3 folds higher than F-5 and F-6, respectively (formulated using PVA 98-99% hydrolyzed, which is a weak emulsifier). The increase in encapsulation efficiency for some of the formulations can be attributed to a decrease in organic phase volume (increased the PLGA concentration) and aqueous phase volume. It should also be noted that increasing PLGA concentration in the organic phase and

reducing the aqueous phase volume did not significantly modify the encapsulation efficiency of formulations F-1 to F-4 (formulated using PVA 87-89% hydrolyzed). However, formulations F-7 and F-8 showed the highest encapsulation efficiency. The formulation conditions and parameters for F-7 and F-8 were similar to F-1 and F-2, respectively, with the only difference being that the organic phase volumes for F-7 and F-8 were lower (higher PLGA concentration) than that of F-1 and F-2. Also, formulations F-5 and F-6 were prepared with a weak emulsifier (PVA, 98-99% hydrolyzed). Thus, formulations F-5 and F-6 show less encapsulation efficiency at PVA concentration as high as 2%. All other formulations were formulated with PVA, 87-89% hydrolyzed, which is a more powerful emulsifier that resulted in higher encapsulation efficiency. Formulations F-3 and F-4 were formulated with 0.2% PVA, 87-89% hydrolyzed and the encapsulation efficiency of both formulations were low; whereas formulations F-1, F-2, F-7 and F-8 formulated with 0.3% PVA, 87-89% hydrolyzed showed higher encapsulation efficiency. Thus, formulations prepared with the same emulsifier type and concentrations showed similar encapsulation efficiency. This also explains the importance of emulsifier grade and concentration in developing stable emulsions with high encapsulation efficiencies.This also explains the importance of emulsifier grade and concentration in developing stable emulsions with high encapsulation efficiencies. Formulations F-7 and F-8 showed the highest encapsulation and loading efficiency; and were optimized for the development of sustained release implant.

4.3.4. Morphological evaluation of microspheres

Under the SEM, dexamethasone-loaded microparticle formulations F1 to F8 appeared spherical with a very smooth surface as shown in Figure 10. SEM images for all the formulations appeared similar without any significant morphological differences.

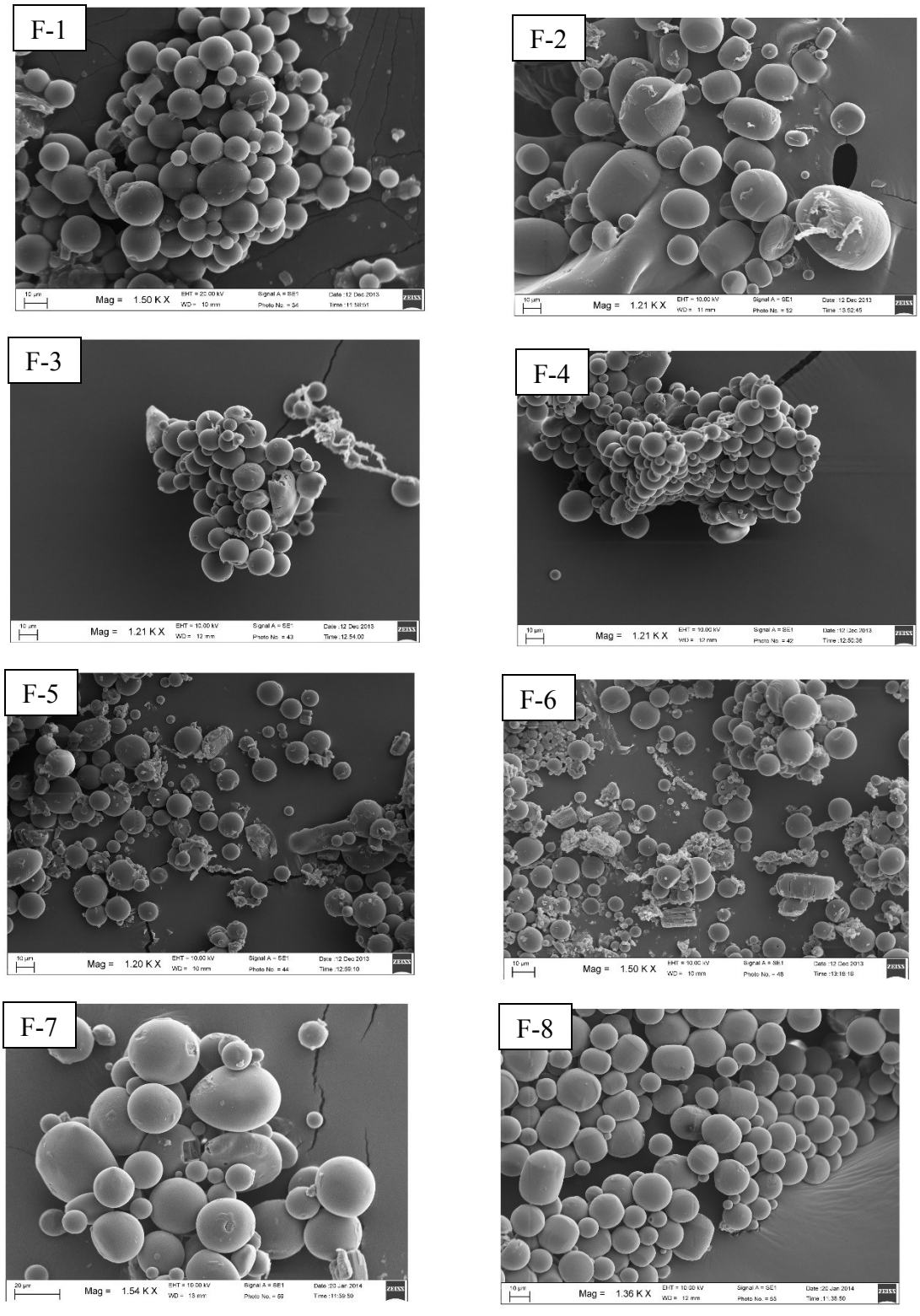

Figure 10 SEM images of dexamethasone-loaded microparticle formulations (F-1 to F-8).

4.3.5. *In vitro* dexamethasone release from microparticles

In vitro release of dexamethasone from microparticle formulations F-1 to F-6 was studied for a period of 8 weeks and a plot of percent cumulative release vs. time was obtained (Figure 11). The studies were done in triplicates and it was observed that the standard deviatons (error bars) were significantly higher for formulations F-1 to F-6 than F-7 and F-8. These studies were performed initially to optimize the release conditions (composition and volume of the release media, sampling time intervals and speed of the shaker incubator). Figure 11 shows that formulations F-1 to F-6 were sustained release. However, varying levels of high initial "burst" drug release were observed. This phenomenon can be attributed to experimental variables and data scaling. For instance, the time scale (x-axis) units were in hours, days and weeks, which was difficult to represent on a graph. Thus, for convenience, the x-axis was represented as time in days. Once the release conditions were optimized, *in vitro* dexamethasone release studies were performed for formulations F-7 and F-8; and a plot of percent cumulative drug release vs time was obtained (Figure 12). Formulations F-7 and F-8 released dexamethasone in a sustained manner. Initial burst release phase was noticed, which may be due to faster release of drug molecules that were adsorbed on the microparticles surfaces or those close to the surfaces. After the initial burst release, which occurred within the first few days, there was a very slow and continuous release of the drug for about 3 months. F-7 released approximately 40% of its drug load at the end of 3 months, whereas F-8 releases approximately 60% of the drug at the end of 3 months.

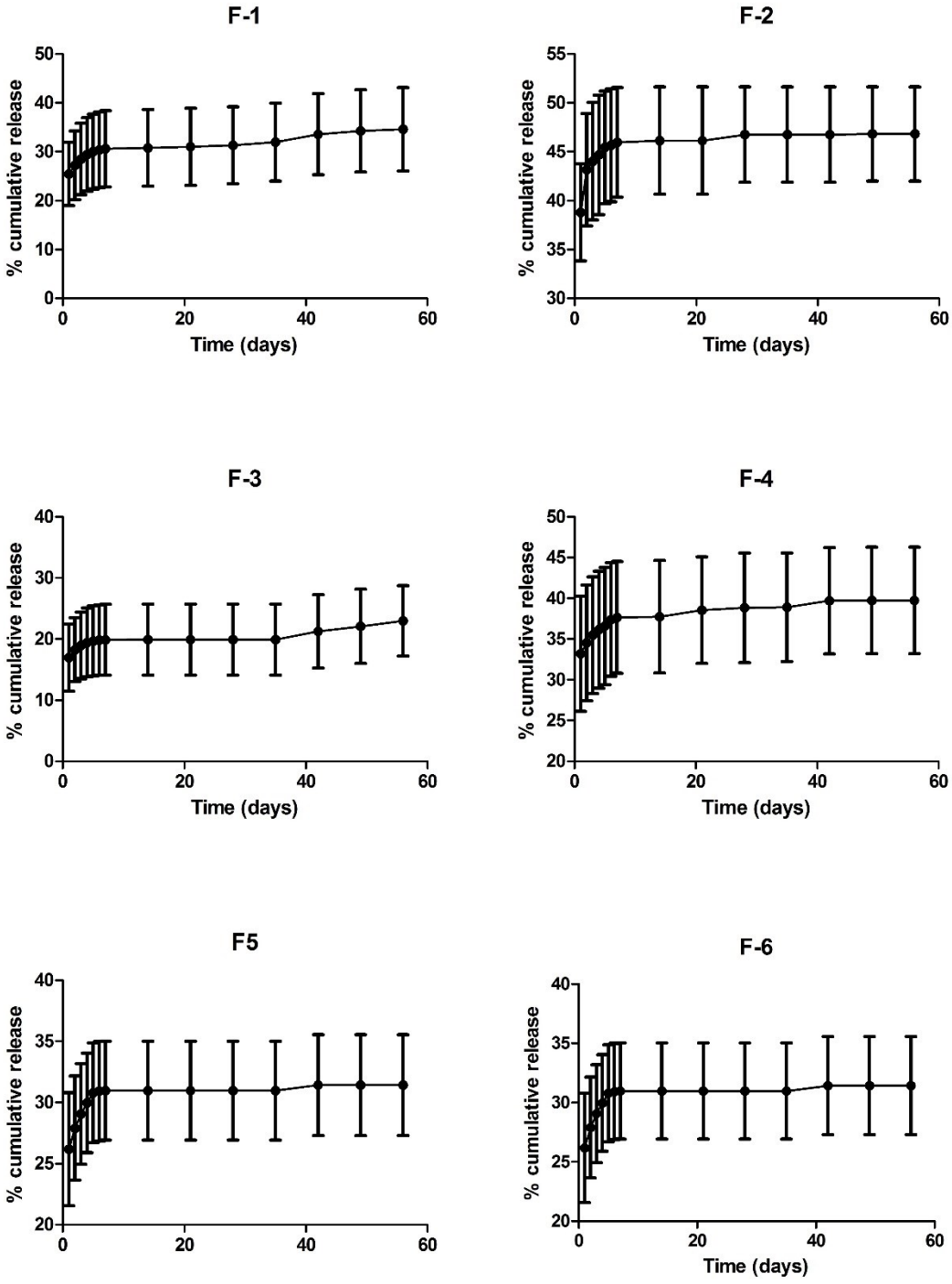

Figure 11 Percent cumulative drug release vs time for dexamethasone-loaded microparticle formulations (F-1 to F-6).

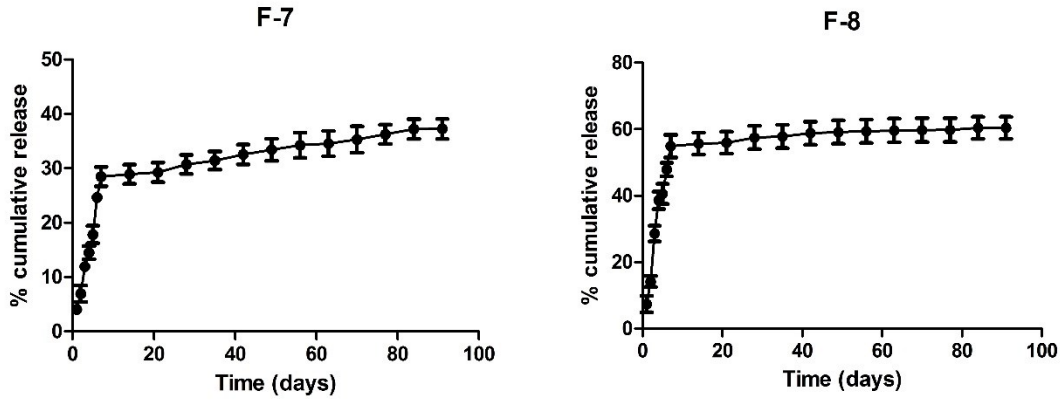

Figure 12 Percent cumulative drug release vs time for dexamethasone-loaded microparticles formulations (F-7 and F-8).

Based on *in vitro* characterization studies of dexamethasone-loaded PLGA microparticles, formulations F-7 and F-8 were optimized for the development of sustained release implant.

4.3.6. X-ray diffraction (XRD) studies

Figure 13 shows the XRD patterns of dexamethasone, PLGA, blank microparticles and dexamethasone-loaded microparticles F-7 and F-8. A plot of intensity (counts) vs 2 theta (2θ°) for dexamethaone drug showed a specific XRD pattern. Specific XRD peaks were absent for PLGA polymer, blank microparticles and dexamethasone-loaded microparticles. Thus, the absence of specific XRD peaks for dexamethasone-loaded microparticles (F-7 and F-8) suggested that dexamethasone was encapsulated within PLGA microspheres.

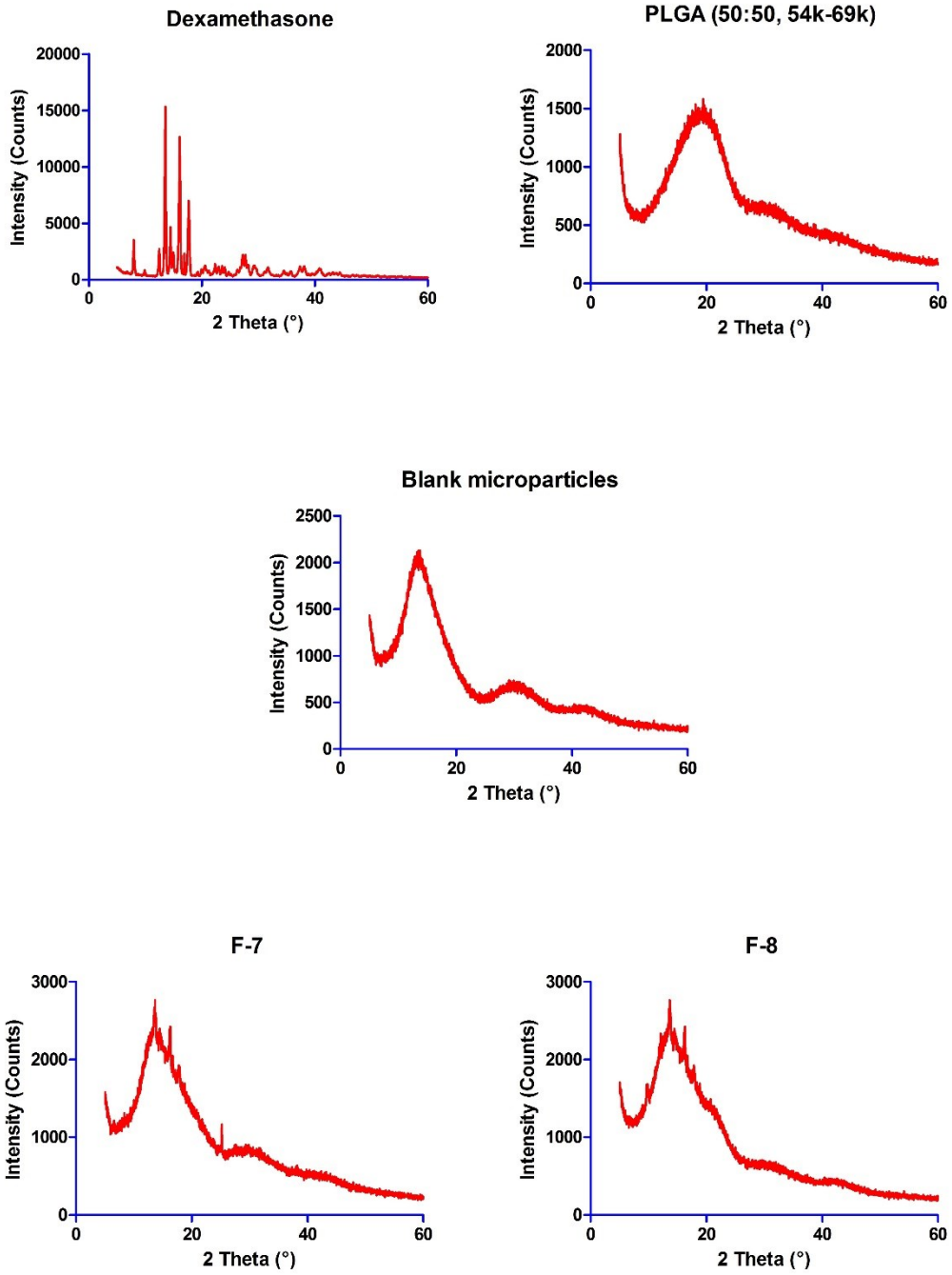

Figure 13 XRD patterns of dexamethasone, PLGA, blank microparticles and dexamethasone-loaded microparticles (F-7 and F-8).

Figure 14 shows the XRD patterns of rhodamine 6G and rhodamine 6G-loaded microparticles. XRD pattern for rhodamine 6G microparticles was similar to PLGA and blank microparticles (Figure 13), whereas rhodamine 6G showed specific XRD peaks. The absence of specific XRD peaks for rhodamine 6G-loaded microparticles confirmed that rhodamine 6G was encapsulated within the PLGA microparticles.

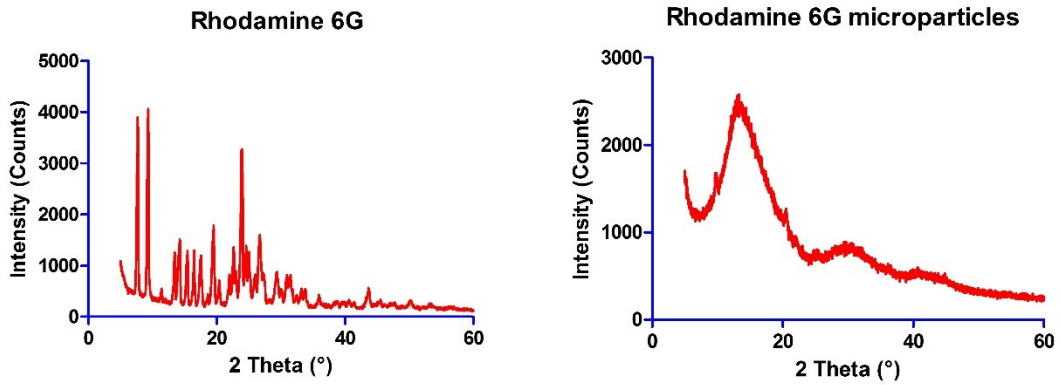

Figure 14 XRD patterns of rhodamine 6G and rhodamine 6G-loaded PLGA microparticles.

4.4. Characterization of alginate sponges

4.4.1. Morphological evaluation of alginate sponges

The calcium alginate sponges were developed as sustained release drug delivery system for dexamethasone-loaded microparticles. These sponges were evaluated for their surface morphology using SEM. SEM images of the alginate sponges formulated with 1 (Figure 15 A) and 2% sodium alginate (Figure 15 B) revealed the highly cross-linked porous nature of the sponges. There were no visual morphological differences between 1 and 2% sodium alginate sponges. The formulated microparticles were much larger than the pore sizes of the sponges and thus, could not be observed within the sponge network.

However, after the sponges were broken down with a spatula the microparticle formulations F-7 and F-8 were released from the sponge network after mechanical disruption of the calcium alginate sponges formulated with 1 and 2% sodium alginate (Figure 16).

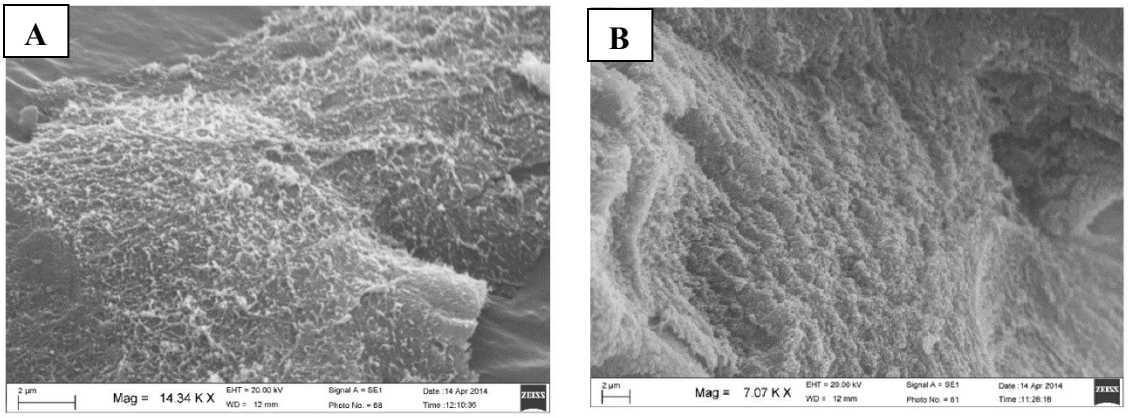

Figure 15 SEM images of calcium alginate sponges prepared with 1 (A) and 2% (B) sodium alginate.

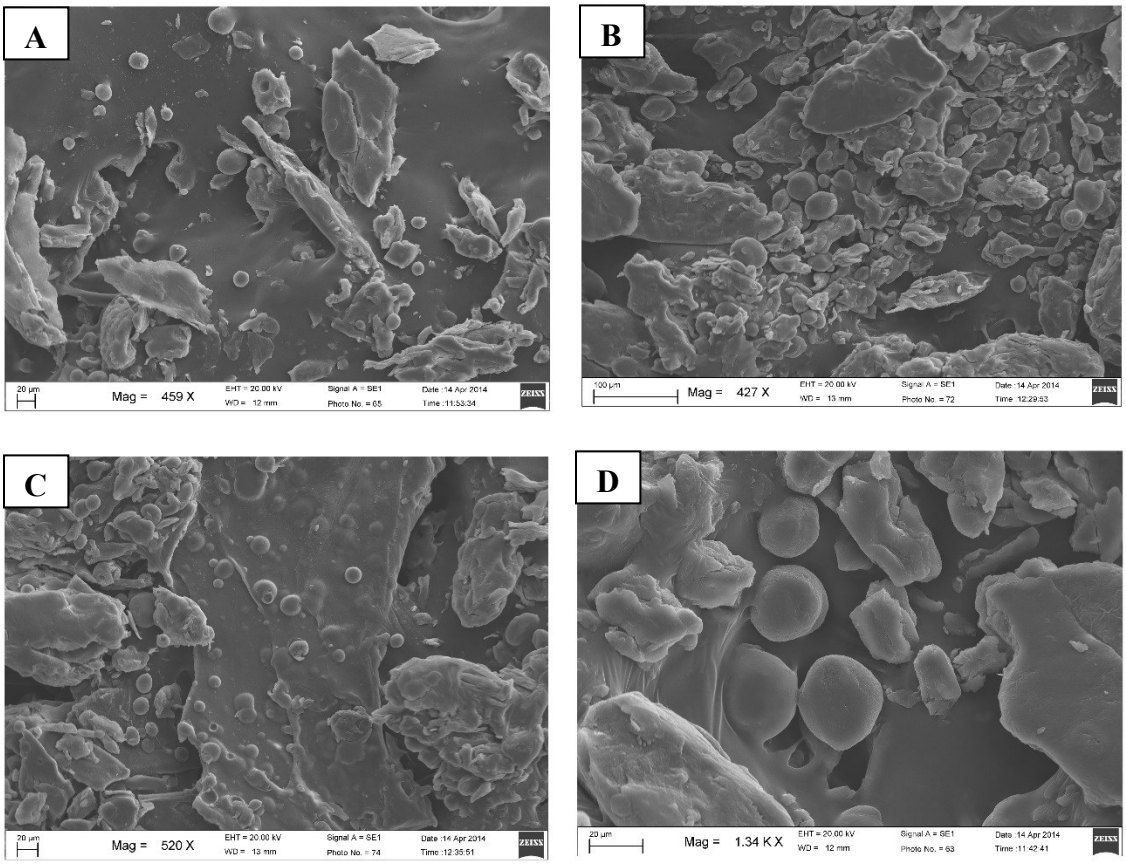

Figure 16 SEM images of microparticles from formulation F-7 released after mechanical disruption of 1 (A) and 2% (B) alginate sponges; and microparticles from formulation F-8 released from 1 (C) and 2% (D) alginate sponges.

4.4.2. Entrapment efficiency of alginate sponges

Microparticles entrapment efficiency of 1 and 2% sodium alginate sponges were determined. The results of the studies are summarized in Table 8**.**

Table 8 Entrapment efficiency of alginate sponges.

Alginate sponge formulation	Entrapment Efficiency (%)
1% sodium alginate (microparticles F-7)	86.74 ± 0.79
2% sodium alginate (microparticles F-7)	91.96 ± 0.83
1% sodium alginate (microparticles F-8)	88.33 ± 0.54
2% sodium alginate (microparticles F-8)	91.22 ± 0.56

It can be observed that sponges prepared with 1% sodium alginate shows entrapment of approximately 86.74% (for sponges prepared with microparticles F-7) and 88.33% (for sponges prepared with microparticles F-8). Also, sponges prepared with 2% sodium alginate showed the entrapment efficiency of 91.96% (for sponges prepared with microparticles F-7) and 91.22% (for sponges prepared with microparticles F-8). All alginate sponges showed good entrapment efficiency. The entrapment efficiency of sponges prepared by 2% sodium alginate was significantly higher than 1% sodium alginate sponges ($P < 0.05$).

4.5. Characterization of chitosan sponges

4.5.1. Morphological evaluation of chitosan sponges

Chitosan based sponges were also developed as sustained release drug delivery system for dexamethasone-loaded microparticles. Surface morphology of the chitosan sponges C3PH5, C3PH6, C6PH5, and C6PH6 were observed under SEM (Figure 17). SEM images of the chitosan sponges revealed a highly cross-linked porous structure. There were no apparent morphological differences in the microstructure and porosity of the four sponge formulations. Figure 18 reveals that the microparticles F-7 were successfully loaded within the chitosan sponge network (C3PH6). The images of F-7

loaded within C3PH5, C6PH5 and C6PH6; and F-8 entrapped within the chitosan sponges does not clearly reveal the microparticles because of much larger mean particle size than the pore sizes of the sponges.

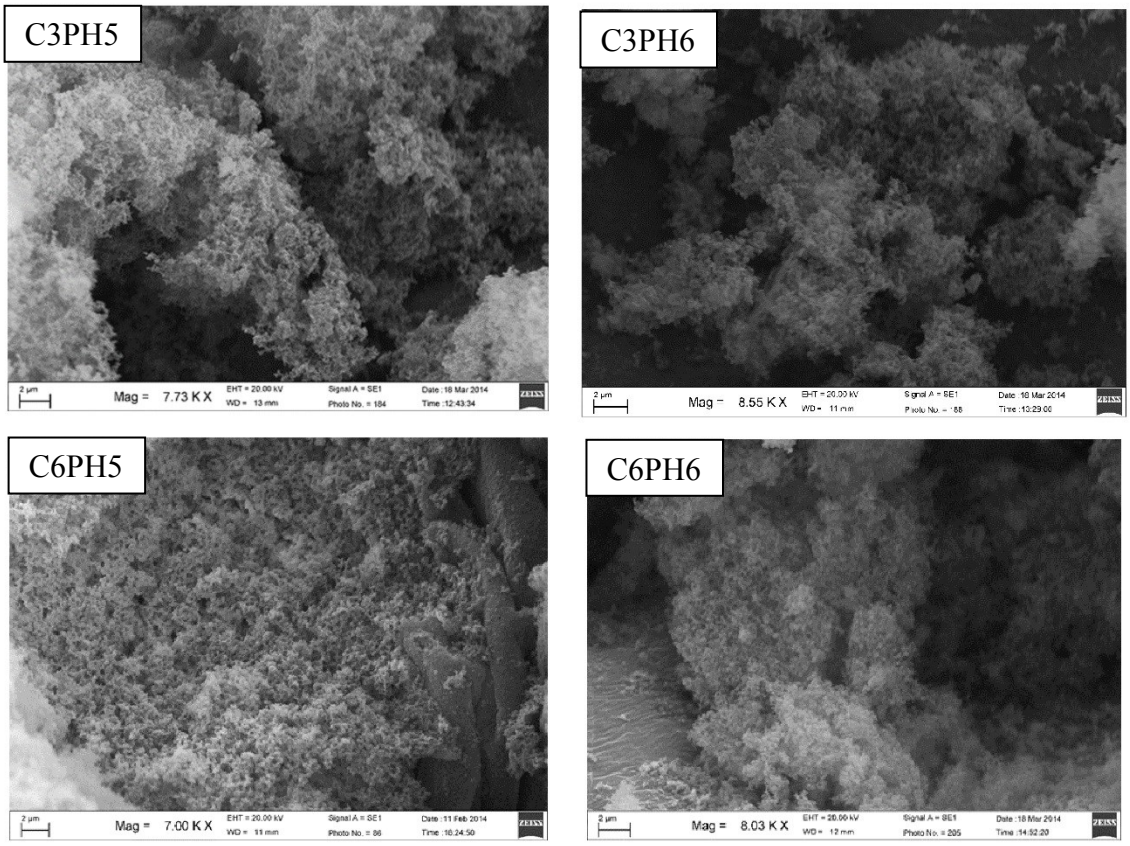

Figure 17 SEM images of chitosan sponges C3PH5, C3PH6, C6PH5 and C6PH6.

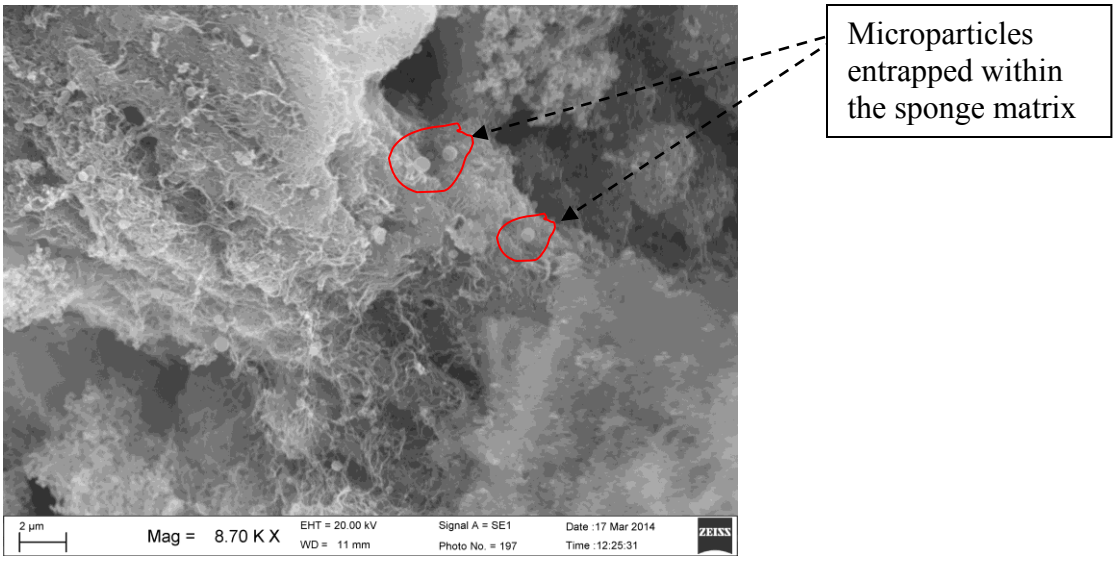

Figure 18 SEM image showing microparticles F-7 entrapped within the chitosan sponge network (C3PH6).

4.6. *In vitro* cellular uptake studies

The purpose of these studies was to determine whether Calu-3 cell line and cultured human nasal cells were capable of taking up PLGA microparticles. Rhodamine 6G dye was used because it was comparable to our model drug. The dye and dexamethasone have similar molecular weight and hydrophobicity. These studies were designed to explore the possible mechanisms of uptake of the microparticles in these cells. Nasal and Calu-3 cell lines showed significantly higher uptake of rhodamine 6G microparticles than free rhodamine 6G dye ($P < 0.05$).

4.6.1. Effect of incubation time on the uptake of rhodamine 6G dye and rhodamine 6G microparticles

Figure 19 shows the effect of incubation time on the uptake of rhodamine 6G dye and rhodamine 6G-loaded microparticles by Calu-3 and nasal cells. It was observed that uptake increased with time and both cells showed maximum uptake at 60 min. Thus, uptake increased upto 60 min, after which no further increase in uptake was observed.

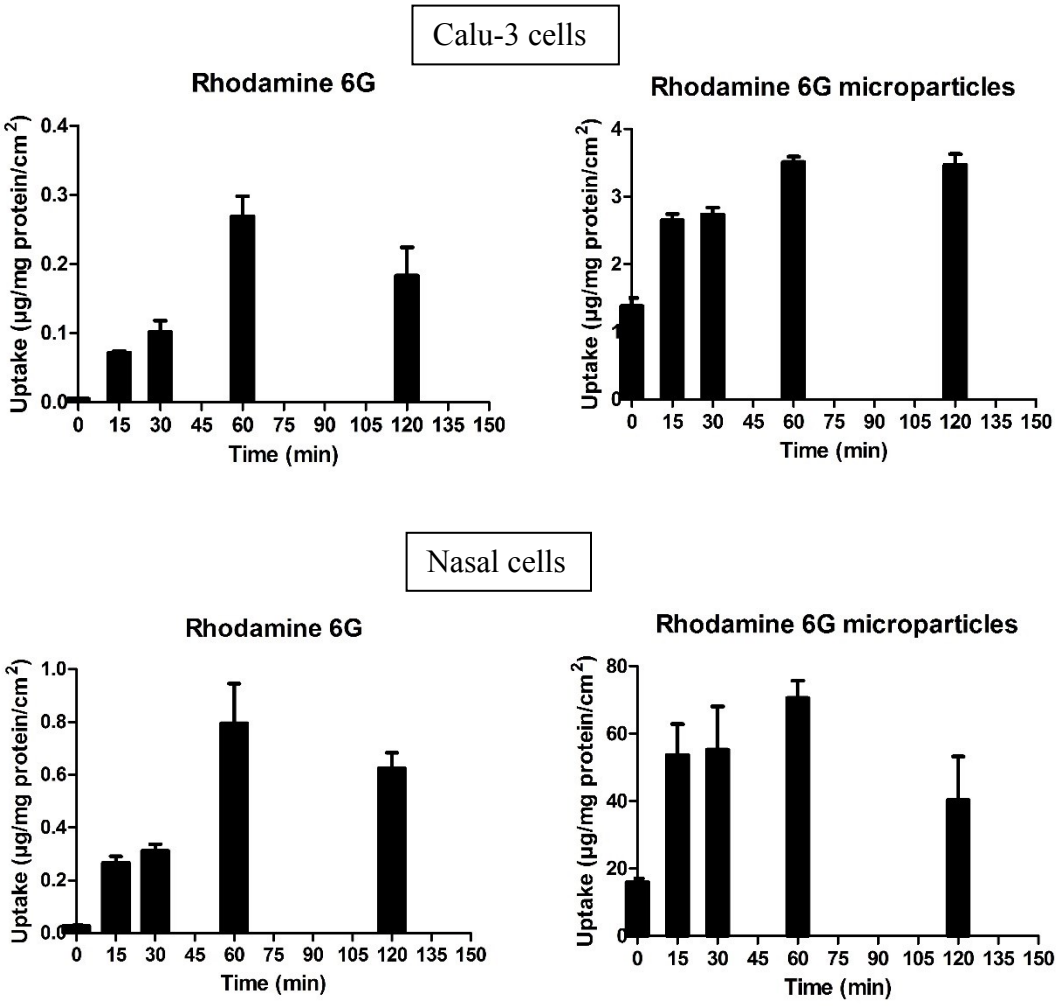

Figure 19 Effect of incubation time on the uptake of rhodamine 6G dye and rhodamine 6G microparticles by Calu-3 cells and nasal cells.

4.6.2. Effect of concentration on the uptake of rhodamine 6G dye and rhodamine 6G microparticles

Figure 20 shows the effect of concentration on the uptake of rhodamine 6G dye and rhodamine 6G-loaded microparticles by Calu-3 and nasal cells. Both cells showed concentration-dependant uptake for free drug, as well as the microparticulate form. Thus, uptake increased with increase in concentration and there was no saturation.

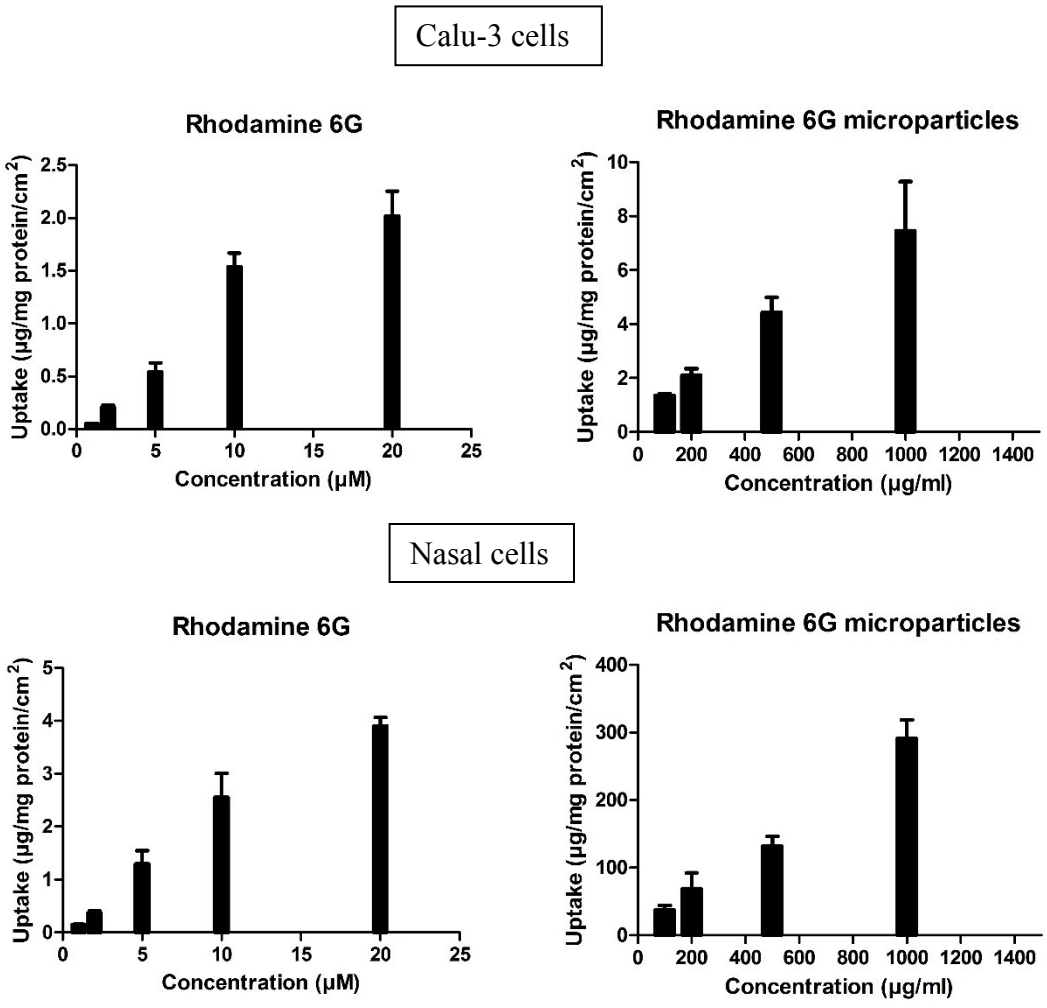

Figure 20 Effect of concentration on the uptake of rhodamine 6G dye and rhodamine 6G microparticles by Calu-3 cells and nasal cells.

4.6.3. Effect of temperature on the uptake of rhodamine 6G dye and rhodamine 6G microparticles

Figure 21 shows the effect of incubation temperature on the uptake of rhodamine 6G dye and rhodamine 6G-loaded microparticles by Calu-3 and nasal cells. Both cells showed that the uptake was higher at 37°C than 4°C for free rhodamine 6G dye and loaded microparticles. This observation points to possible uptake by an active transport process.

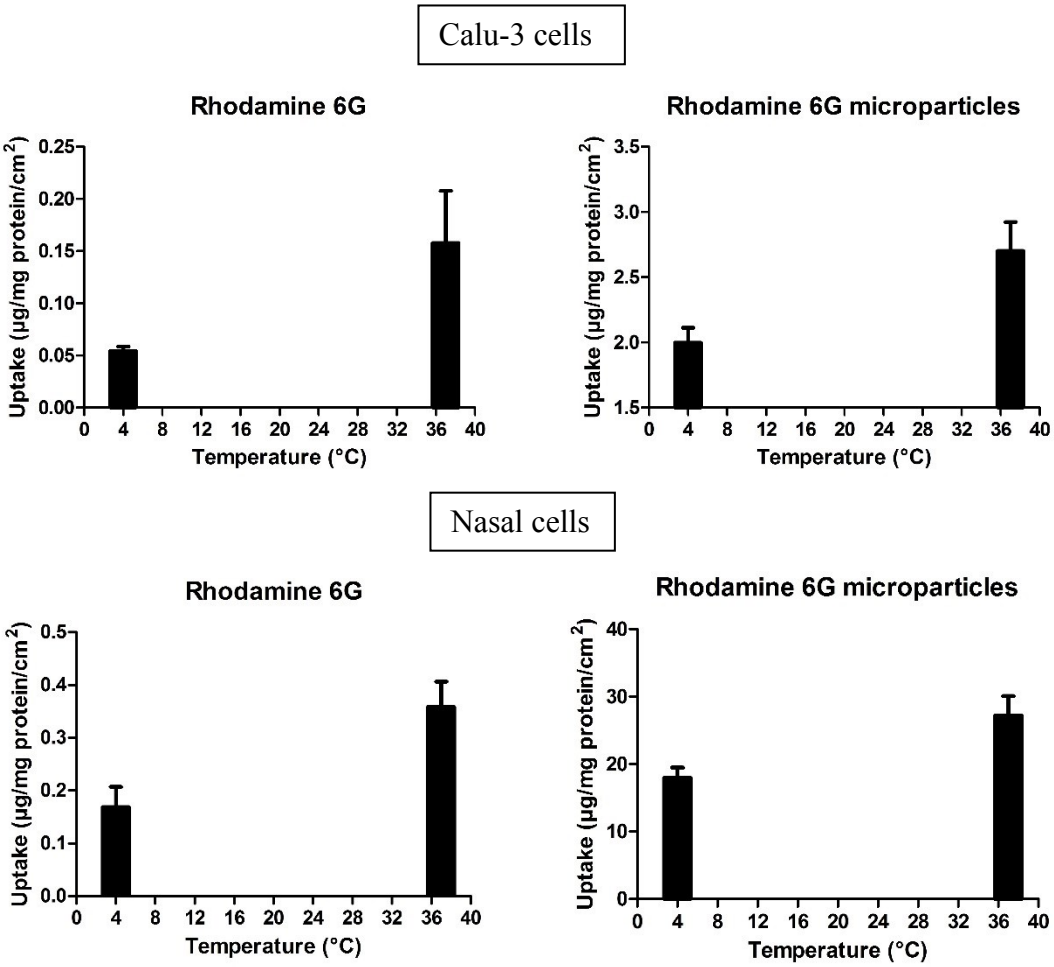

Figure 21 Effect of incubation temperature on the uptake of rhodamine 6G dye and rhodamine 6G microparticles by Calu-3 cells and nasal cells.

4.6.4. Effect of pH on the uptake of rhodamine 6G dye and rhodamine 6G microparticles

Figure 22 shows the effect of pH on the uptake of rhodamine 6G dye and rhodamine 6G-loaded microparticles by Calu-3 and nasal cells. It was observed that both cells showed maximum uptake at physiological pH 7.4 for free rhodamine 6G dye and rhodamine 6G-loaded microparticles. The uptake was lowest at pH 5.5.

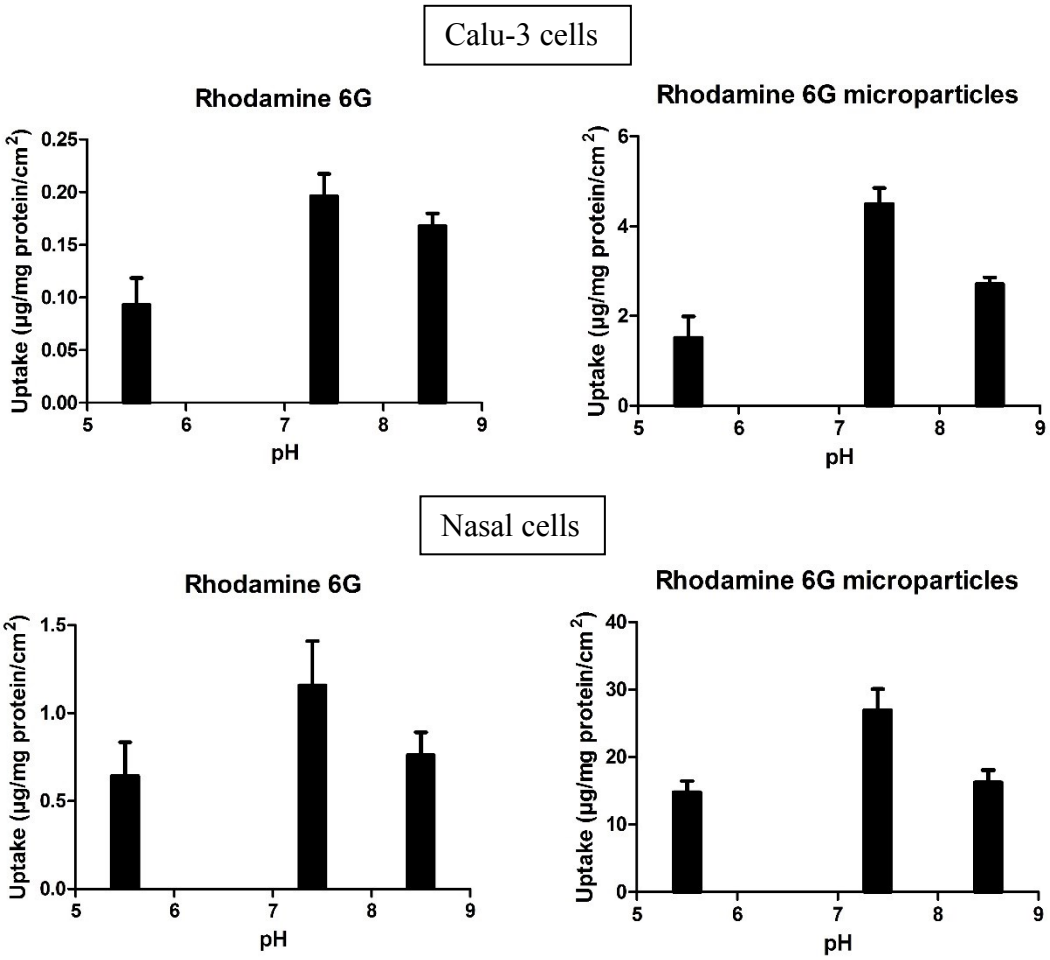

Figure 22 Effect of pH on the uptake of rhodamine 6G dye and rhodamine 6G microparticles by Calu-3 cells and nasal cells.

CHAPTER 5 DISCUSSION

The aim of the studies described in this thesis was to conduct proof-of-principles studies necessary to develop a novel sustained release biodegradable drug delivery system for treatment of chronic rhinosinusitis. Chronic sinusitis may require local drug targeting for a prolonged period of time. It is very challenging to develop a drug delivery system, which can release targeted drug locally to the affected sinuses for 2 to 6 months. PLGA was chosen as the biodegradable poymer for this project because it has been approved by the US Food and Drug Administration (FDA) and Health Canada for use in humans. The polymer also has a very slow degradation rate and degrades slowly over a period of about 6 months. Thus, encapsulating the corticosteroid, dexamethasone in the PLGA matrix for possible sustained release into the sinuses was deemed a novel strategy for treating chronic sinusitis with recurrent polyps.

5.1. Analytical method development and validation

Reversed-phase liquid chromatography was chosen for the detection and quantification of dexamethasone as it gave acceptable linearity with drug elution at 1.40 min. Repeatability and inter-day studies designed to detect the precision of the method confirmed the reproducibility of the assay method (CV < 5 %) for intra-day and inter-day precision studies. Furthermore, the HPLC method was accurate as the percentage recovery of dexamethasone was within 95 % - 105 % range (acceptable range for early drug development). The relative standard deviation was less than 1%, which was also within the acceptance criteria limits for accuracy studies[69]. The analytical method was

accurate and precise for the detection and quantification of dexamethasone. Based on these findings, subsequent studies were conducted with the assurance that drug detection and quantification would not negatively affect the experimental data.

5.2. Characterization and optimization of microparticle formulations

Blank microparticles (without dexamethasone) were formulated using PLGA. These formulations were used to study the polymer degradation over a period of more than 3 months. PLGA is a copolymer of lactic acid and glycolic acid. When microparticles are suspended in a buffer of pH 7.4, there is a decrease in pH with time because the degradation products of PLGA (lactic acid and glycolic acid) are acidic[70,71]. Dexamethasone-loaded PLGA microparticles of size 1.5 to 2.0 μm were developed and characterized. PVA was chosen as the emulsifier because the hydroxyl groups in PVA interact with the water phase and the vinyl chains interact with dichloromethane to give a stable emulsion. However, the emulsifier grade and its optimum concentration was crucial for developing a stable microparticles emulsion[72,73]. Thus, different grades and concentrations of PVA were used for optimizing the microparticle formulations. For our studies, we used two grades of PVA; 98-99% hydrolyzed (MW 31k to 50k) and 87-89% hydrolyzed (MW 13k to 23k). PVA 87-89% hydrolyzed is a more powerful emulsifier and a stable emulsion was obtained at a concentration as low as 0.2%. Much higher concentration of PVA 98-99% hydrolyzed (2%) was needed for a stable emulsion. Emulsifier concentration and particle size are inversely related. Higher emulsifier concentrations result in smaller microparticles. Particle size also depends on drug

concentration, organic phase volume, aqueous phase volume and organic to aqueous phase ratio[73]. At higher drug concentration, particle size increases, thus increasing drug encapsulation efficiency. This explains the highest mean particles size for formulations F-7 and F-8. Also, these formulations showed the highest encapsulation efficiency. However, excessively high concentrations of the emulsifier may lead to toxicity due to residual PVA. Residual PVA affects the physical properties of the microparticles and the cellular uptake[74]. At lower concentrations of PVA, the PLGA is precipitated out due to instability. Thus, it was a challenge to optimize the ideal conditions for developing microparticles. Based on the mean particles size, encapsulation and loading efficiency, conditions for formulations F-7 and F-8 were ideal. Also, morphological evaluation using SEM revealed smooth spherical surfaces of dexamethasone-loaded microparticles. *In vitro* drug release from formulations F-7 and F-8 showed a linear drug release profile of 25% and 40%, respectively for upto 1 week, with an initial burst release of 4% and 7%, respectively within 24 hours. After 1 week, the drug was released from the microparticles slowly in a sustained manner, releasing 40% and 60% of the drug from formulations F-7 and F-8, respectively at the end of 3 months. Thus, drug release from the microparticles showed a biphasic pattern, with faster initial drug release, followed by sustained drug release. Non-encapsulated drug particles could not be seen on the surfaces of the smooth spherical microparticles (SEM images). This implies that the initial fast release of the drug may not be attributed to drug presence on the surface of the particles. Also, smooth surfaces indicated the absence of macropores on the microparticle surfaces. However, the presence of nanopores which may not be visualized with SEM might contribute to the initial faster drug release, as the molecular form of the drug can escape through these

nanopores[75]. Owing to water imbibtion on exposure to the release media, the surface pores are closed leading to a diffusion barrier[75]. Dexamethasone, being a highly hydrophobic drug can not readily escape through this aqueous diffusion barrier or water filled cavities. This explains the sustained release period of dexamethasone from the microparticles. After the initial release period, drug release was mainly dependant on drug diffusion through the polymer matrix and the degradation of the polymer network. X-ray diffraction (XRD) studies were performed to confirm that dexamethasone was encapsulated within the microparticles. XRD patterns for drug-loaded microparticles were similar to PLGA and blank microparticles and specific dexamethasone peaks were absent. If the drug was not encapsulated within the PLGA matrix, then the XRD pattern for dexamethasone-loaded microparticles would correspond to dexamethasone.

5.3. Characterization and formulation of alginate and chitosan sponges as potential delivery systems for microparticles

5.3.1. Calcium alginate sponges

Calcium alginate sponges can be potentially used as a drug delivery system for drug-loaded microparticles. Sodium alginate 1 and 2% solutions when cross-linked with 1% calcium chloride solution forms a hydrogel, which on drying resulted in a sponge. These sponges showed high entrapment efficiency of microparticles and were examined under the SEM, which revealed the highly cross-linked porous network. SEM images also showed the presence of microparticles in the sponge which was an indication of the successful entrapment of the microparticles in the sponge network. However, owing to nano-sized pores of the alginate sponges and larger microparticle size (2 μm), it is

unlikely that the microparticles entrapped within the sponge matrix would leak and release through the sponge structure. Alginate sponges would have to degrade first before the release of microparticles. The drug release from the microparticles was determined to take more than three months. Thus, drug release from the sponge (implant) may have a lag phase of a few weeks, within which little or no drug is released. A possible alternative which can be explored is an *in situ* gelation method. Calcium chloride solution, on addition to sodium alginate solution gives a translucent calcium alginate hydrogel. If, one side of a double barrel syringe contains microparticles suspended in sodium alginate solution and the other side of the syringe contains calcium chloride solution, mixing both solutions just before injection to the affected sinus mucosa can form an *in situ* gelling hydrogel implant containing drug-loaded microparticles.

5.3.2. Chitosan sponges

Chitosan sponges were developed in collaboration with McGill University, Montréal, QC, Canada[68]. Researchers at McGill University have successfully developed and evaluated GDP cross-linked chitosan sponges as scaffolds for drug delivery applications. We explored the chitosan-based sponges as a possible delivery system for dexamethasone-loaded microparticles. We evaluated the sponges for surface morphology using SEM, which revealed the intense cross-linking and porosity. However, as the mean particle size of the microparticles was higher (approximately 2 μm) than the pore sizes of the chitosan sponges (nanosized), it was unlikely that the microparticles entrapped within the sponge matrix would leak through the sponge structure. *In vivo*, chitosan sponges have to be degraded to release the entrapped microparticles; which in turn degrades to

release the drug (dexamethasone) to its site of action. Thus, similar to the alginate sponges, drug release from the chitosan sponge may also have an initial lag phase, within which little or no drug is released. Chitosan sponges can also be further explored for *in situ* sponge formation. One side of the double barrel syringe may contain microparticles suspended in chitosan solution, whereas the other side contains GDP solution. Mixing both solutions just before injection can result in an *in situ* implant in the form a of a white coloured opague sponge, which contains the entrapped microparticles.

For alginate hydrogel and chitosan sponges, the *in situ* gelling implant may have considerable advantages. There may be faster drug release from "non-entrapped" microparticles and hence, reduction in the initial lag phase. Also, as the implants are moistened, the microparticles release is expected to be faster and more consistent, owing to the uniform water uptake. This may be due to reduction of glass transition temperature (Tg) of the moist polymer, which results in increased elasticity and rubbery state of the polymer. This explains the plasticizing nature of water[75]. Thus, the microparticles are expected to have higher diffusivity through the wet polymer. On the other hand, if dried sponges are implanted, drug release is expected to be considerably slower as the sponge polymer are in a glass state (rigid), owing to higher glass transition temperature (Tg)[75]. Moreover, as the sinuses are air filled cavities, with mucous as the source of moisture, dried sponges may rely on the presence of blood and mucous for any water imbibtion and subsequent drug release. Thus, *in situ* gelation method could be a more feasible option that warrants exploration in future studies.

Although alginate and chitosan sponges are promising delivery systems for sustained release microparticles for possible treatment of some chronic sinusitis, further

evaluations are required. The concentration of microparticles to be incorporated into the delivery system needs to be optimized. Very high concentrations may interfere with cross-linking of the sponges, whereas very low concentrations may result in an initial lag phase within which little or no drug is released, which is undesirable for patients requiring immediate treatment.

5.4. *In vitro* cellular uptake studies

Rhodamine 6G-loaded PLGA microparticles showed significantly higher ($P < 0.05$) uptake than non-encapsulated free rhodamine 6G dye by Calu-3 and nasal cells. Organic Cation Transporters (OCT) is the primary mechanism of uptake for rhodamine 6G dye[76,77,78]. Rhodamine 6G may also be taken up by passive diffusion[79,80] but it is a substrate for P-glycoprotein efflux protein[80]. The possible mechanisms of uptake for particles through biological barriers include paracellular (for particle size < 0.050 μm), endocytosis (for particle size < 0.5 μm)[81] and lymphatic uptake (for particles of size 0.01 - 0.1 μm). Particles larger than 0.1 μm can be absorbed by the lymphatic system but at a very slow rate[82]. Rhodamine microparticles used for these studies were between 0.2 to 0.3 μm, and thus the nasal and Calu-3 cellular uptake of these particles could be through endocytosis. Also, rhodamine microparticles were much smaller than dexamethasone microparticles (1.50 to 2.00 μm). Cellular uptake of microparticles is size dependant and decreases with increase in particle size[81,83]. It was demonstrated in a Caco-2 cell model that the uptake of 0.1 μm PLGA microparticles was approximately 2.5 fold higher than 1 μm particles and 6-fold higher than 10 μm particles[81]. Thus, the extent of dexamethasone microparticles uptake is expected to be less compared to the smaller diameter rhodamine

microparticles. This implies that in future studies efforts will be made to lower the particle sizes of the formulations. Therefore, more work is required in terms of particle reduction and polymer modification.

CHAPTER 6 CONCLUSIONS

The objective of this study was to develop novel sustained release drug delivery system for the treatment of chronic sinusitis. We developed dexamethasone-loaded PLGA microparticles which released the drug over a period of 3 months. However, we needed to incorporate these microparticles into a delivery system for local targeting to the affected sinuses. Thus, we explored the possibility of entrapping these drug-loaded microparticles in alginate or chitosan based sponge network, which can be implanted in the affected sinuses, following FESS. Significant findings from our studies were that PLGA can be successfully used as a biodegradable polymer for development of drug-loaded microparticles, which can release loaded drug over 2 to 6 months period. Formulated micropartciles were successfully entrapped in a sponge network which can be developed as sustained release implant. Despite the reasonable success that we achieved in this project, further studies are needed to evaluate the concentration of microparticles in the sponges necessary for optimal drug loading and release. *In situ* gelation/sponge formation can be explored as a feasible approach for delivery of the microparticles. Some *in vivo* studies in rabbits[84],[85] will be used in the future to evaluate drug release from dried sponge as well as from the *in situ* gel/sponge formation. Cellular uptake studies of rhodamine 6G-loaded PLGA microparticles also gave useful data regarding the uptake of PLGA-based microparticles in cultured human nasal epithelial and Calu-3 cells. The data indicated that microparticles released from the sponge/hydrogel are expected to be readily taken up by the nasal and sinus mucosa epithelial cells *in vivo*.

Taken together the data from this research project suggests that dexamethasone-loaded PLGA microparticles can be used to develop promising next generation implants for recalcitrant chronic sinusitis.

BIBLIOGRAPHY

[1] Watelet, J.B.; van Cauwenberge, P. Applied anatomy and physiology of the nose and paranasal sinuses. *Allergy*. **1999**, *54*, 14–25.

[2] Van Cauwenberge, P.; Sys, L.; de Belder, T.; Watelet, J.B. Anatomy and physiology of the nose and the paranasal sinuses. *Immunol. Allergy Clin. N. Am*. **2004**, *24*, 1–17.

[3] Jones, N. The nose and paranasal sinuses physiology and anatomy. *Adv. Drug Deliv. Rev*. **2001**, *51*, 5–19.

[4] Singh, A. Paranasal sinus anatomy. Available online: http://emedicine.medscape.com/article/1899145-overview (accessed on 09 January 2014).

[5] Gupta, A.; Mercurio, E.; Bielamowicz, S. Endoscopic inferior turbinate reduction: An outcomes analysis. *Laryngoscope.* **2001**, *111*, 1957–1959.

[6] Tan, B.K.; Zirkle, W.; Chandra, R.K.; Lin, D.; Conley, D.B.; Peters, A.T.; Grammer, L.C.; Schleimer, R.P.; Kern, R.C. Atopic profile of patients failing medical therapy for chronic rhinosinusitis. *Int. Forum Allergy Rhinol.* **2011**, *1*, 88–94.

[7] Al Badaai, Y.; Samaha, M. Outcome of endoscopic sinus surgery for chronic rhinosinusitis patients: A Canadian experience. *J. Laryngol. Otol.* **2010**, *124*, 1095–1099.

[8] Chan, Y.; Kuhn, F.A. An update on the classifications, diagnosis, and treatment of rhinosinusitis. *Curr. Opin. Otolaryngol. Head Neck Surg.* **2009**, *17*, 204–208.

[9] Guilemany, J.M.; Alobid, I.; Mullol, J. Controversies in the treatment of chronic rhinosinusitis. *Expert Rev. Respir. Med.* **2010**, *4*, 463–477.

[10] Jarvis, D.; Newson, R.; Lotvall, J.; Hastan, D.; Tomassen, P.; Keil, T.; Gjomarkaj, M.; Forsberg, B.; Gunnbjornsdottir, M.; Minov, J.; *et al.* Asthma in adults and its association with chronic rhinosinusitis: The GA2LEN survey in Europe. *Allergy.* **2012**, *67*, 91–98.

[11] Ferguson, B.J.; Otto, B.A.; Pant, H. When surgery, antibiotics, and steroids fail to resolve chronic rhinosinusitis. *Immunol. Allergy Clin. N. Am.* **2009**, *29*, 719–732.

[12] Sedaghat, A.R.; Gray, S.T.; Wilke, C.O.; Caradonna, D.S. Risk factors for development of chronic rhinosinusitis in patients with allergic rhinitis. *Int. Forum Allergy Rhinol.* **2012**, *2*, 370–375.

[13] Wagner, W. Changing diagnostic and treatment strategies for chronic sinusitis. *Cleve Clin J Med*. **1996**, 63, 396-405.

[14] Brook, I.; Hinthorn, D.R. Chronic sinusitis medication. Available online: http://emedicine.medscape.com/article/232791-medication#showall (accessed on 09 August 2014).

[15] Côté, D.W.; Wright, E.D. Triamcinolone-impregnated nasal dressing following endoscopic sinus surgery: A randomized, double-blind, placebo-controlled study. *Laryngoscope.* **2010**, *120*, 1269–1273.

[16] Albu, S. Novel drug-delivery systems for patients with chronic rhinosinusitis. *Drug Des. Devel. Ther*. **2012**, *6*, 125–132.

[17] Durand, M.; le Guellec, S.; Pourchez, J.; Dubois, F.; Aubert, G.; Chantrel, G.; Vecellio, L.; Hupin, C.; de Gersem, R.; Reychler, G.; *et al.* Sonic aerosol therapy to target maxillary sinuses. *Eur. Ann. Otorhinolaryngol. Head Neck Dis.* **2012**, *129*, 244–250.

[18] Chronic Sinusitis. Available online: http://www.patient.co.uk/health/Sinusitis-Chronic.htm (accessed on 30 November 2013).

[19] Lin, D.C.; Chandra, R.K.; Tan, B.K.; Zirkle, W.; Conley, D.B.; Grammer, L.C.; Kern, R.C.; Schleimer, R.P.; Peters, A.T. Association between severity of asthma and degree of chronic rhinosinusitis. *Am. J. Rhinol. Allergy.* **2011**, *25*, 205–208.

[20] Available online: http://www.accessdata.fda.gov/cdrh_docs/pdf10/P100044b.pdf (accessed on 09 August 2014).

[21] MedlinePlus. Stent. Available online: http://www.nlm.nih.gov/medlineplus/ency/article/002303.htm (accessed on 18 March 2014).

[22] US Food and Drug Administration. Medical Devices. Available online: http://www.fda.gov/MedicalDevices/DeviceRegulationandGuidance/HowtoMarketYourDevice/InvestigationalDeviceExemptionIDE/ucm046698.htm (accessed on 17 March 2014).

[23] Zilberman, M.; Kraitzer, A.; Grinberg, O.; Elsner, J.J. Drug-eluting medical implants. *Handb. Exp. Pharmacol.* **2010**, *197*, 299–341.

[24] Park, J.B.; Lakes, R.S. Soft Tissue Replacement-II: Blood Interfacing Implants. In *Biomaterials an Introduction*, 3rd ed.; Springer: New York, NY, USA, 2007; pp. 331–367.

[25] Biomedical Implants. Available online: http://www.bmecentral.com/implants.html (accessed on 24 December 2013).

[26] Sclafani, A.P. Nasal Implants. Available online: http://emedicine.medscape.com/article/843111-overview (accessed on 18 October 2013).

[27] Sinusitis-Treatment. Available online: http://www.nhs.uk/Conditions/Sinusitis/Pages/Treatment.aspx (accessed on 23 December 2013).

[28] Steroid Nasal Sprays. Available online: http://www.patient.co.uk/health/steroid-nasal-sprays (accessed on 14 January 2013).

[29] König, A.; Schiele, T.M.; Rieber, J.; Theisen, K.; Mudra, H.; Klauss, V. Influence of stent design and deployment technique on neointima formation and vascular remodeling. *Z. Kardiol.* **2002**, *91*, 98–102.

[30] Waksman, R. Biodegradable stents: They do their job and disappear. *J. Invasive Cardiol.* **2006**, *18*, 70–74.

[31] Cutlip, D.; Abbott, J.D. Drug-Eluting Compared to Bare Metal Intracoronary Stents. Available online: http://www.uptodate.com/contents/drug-eluting-compared-to-bare-metal-intracoronary-stents (accessed on 19 October 2013).

[32] Virmani, R.; Farb, A.; Guagliumi, G.; Kolodgie, F.D. Drug-eluting stents: Caution and concerns for long-term outcome. *Coron. Artery Dis.* **2004**, *15*, 313–318.

[33] Hickey, T.; Kreutzer, D.; Burgess, D.J.; Moussy, F. Dexamethasone/PLGA microspheres for continuous delivery of an anti-inflammatory drug for implantable medical devices. *Biomaterials.* **2002**, *23*, 1649–1656.

[34] Bhardwaj, U.; Sura, R.; Papadimitrakopoulos, F.; Burgess, D.J. PLGA/PVA hydrogel composites for long-term inflammation control following s.c. implantation. *Int. J. Pharm.* **2010**, *384*, 78–86.

[35] Margolis, J.R. The excel stent: A good DES, but can we really stop clopidogrel after 6 months? *JACC Cardiovasc. Interv.* **2009**, *2*, 310–311.

[36] Uurto, I.; Mikkonen, J.; Parkkinen, J.; Keski-Nisula, L.; Nevalainen, T.; Kellomäki, M.; Törmälä, P.; Salenius, J.P. Drug-eluting biodegradable poly-D/L-lactic acid vascular stents: An experimental pilot study. *J. Endovasc. Ther.* **2005**, *12*, 371–379.

[37] Makadia, H.K.; Siegel, S.J. Poly lactic-co-glycolic Acid (PLGA) as biodegradable controlled drug delivery carrier. *Polymers* **2011**, *3*, 1377–1397.

[38] Lai, S.K.; Suk, J.S.; Pace, A.; Wang, Y.Y.; Yang, M.; Mert, O.; Chen, J.; Kim, J.; Hanes, J. Drug carrier nanoparticles that penetrate human chronic rhinosinusitis mucus. *Biomaterials* **2011**, *32*, 6285–6290.

[39] Med-Tech Innovation. Drug-Eluting Bioresorbable Stents. Available online: http://www.med-techinnovation.com/Articles/articles/article/25 (accessed on 10 July 2013).

[40] Gao, S.Q.; Maeda, T.; Okano, K.; Palczewski, K. A microparticle/hydrogel combination drug-delivery system for sustained release of retinoids. *Invest. Ophthalmol. Vis. Sci.* **2012**, *53*, 6314–6323.

[41] Schramm, C.; Spitzer, M.S.; Henke-Fahle, S.; Steinmetz, G.; Januschowski, K.; Heiduschka P.; Geis-Gerstorfer, J.; Biedermann, T.; Bartz-Schmidt, K.U.; Szurman, P. The cross-linked biopolymer hyaluronic acid as an artificial vitreous substitute. *Invest. Ophthalmol. Vis. Sci.* **2012**, *53*, 613–621.

[42] Wang, Y.; Wei, Y.T.; Zu, Z.H.; Ju, R.K.; Guo, M.Y.; Wang, X.M.; Xu, Q.Y.; Cui, F.Z. Combination of hyaluronic acid/hydrogel scaffold and PLGA microspheres for supporting survival of neural stem cells. *Pharm. Res.* **2011**, *28*, 1406–1414.

[43] Xu, L.; Zhang, X.; Zhu, C.; Zhang, Y.; Fu, C.; Yang, B.; Tao, L.; Wei, Y. Nonionic polymer cross-linked chitosan hydrogel: preparation and bioevaluation. *J. Biomater. Sci. Polym. Ed.* **2013**, *24*, 1564–1574.

[44] Mayo Clinic. Chronic Sinusitis. Available online: http://www.mayoclinic.org/diseases-conditions/chronic-sinusitis/basics/treatment/con-20022039 (accessed on 10 August 2013).

[45] Bednarski, K.A.; Kuhn, F.A. Stents and drug-eluting stents. *Otolaryngol Clin North Am*. **2009**, *42*, 857-866.

[46] Tan, B.K.; Lane, A.P. Endoscopic sinus surgery in the management of nasal obstruction. *Otolaryngol Clin North Am*. **2009**, *42*, 227–240.

[47] Kuhn, F.A.; Church, C.A.; Goldberg, A.N.; Levine, H.L.; Sillers, M.J.; Vaughan, W.C.; Weiss, R.L. Balloon catheter sinusotomy: one-year follow-up - outcomes and role in functional endoscopic sinus surgery. *Otolaryngol Head Neck Surg.* **2008**, *139*, S27-37.

[48] Removal of nasal adhesions. Surgery overview. Available online: http://www.webmd.com/a-to-z-guides/removal-of-nasal-adhesions-surgery-overview (accessed on 30 November 2013).

[49] Weitzel, E.K.; Wormald, P.J. A scientific review of middle meatal packing/stents. *Am J Rhinol.* **2008**, *22*, 302-307.

[50] Weber, R.; Hochapfel, F.; Draf, W. Packing and stents in endonasal surgery. *Rhinology.* **2000**, *38*, 49-62.

[51] Murr, A.H.; Smith, T.L.; Hwang, P.H.; Bhattacharyya, N.; Lanier, B.J.; Stambaugh, J.W.; Mugglin, A.S. Safety and efficacy of a novel bioabsorbable, steroid eluting sinus stent. *Int Forum Allergy Rhinol.* **2011,** *1*, 23-32.

[52] Desrosiers, M.; Evans, G.A.; Keith, P.K.; Wright, E.D.; Kaplan, A.; Bouchard, J.; Ciavarella, A.; Doyle, P.W.; Javer, A.R.; Leith, E.S.; Mukherji, A.; Schellenberg, R.; Small, P.; Witterick, I.J. Canadian clinical practice guidelines for acute and chronic rhinosinusitis. *J Otolaryngol Head Neck Surg.* **2011**, *40*, S99-193.

[53] Li, P.M.; Downie, D.; Hwang, P.H. Controlled steroid delivery via bioabsorbable stent: safety and performance in a rabbit model. *Am J Rhinol Allergy.* **2009**, *23*, 591-596.

[54] Kennedy, D.W. The PROPEL™ steroid-releasing bioabsorbable implant to improve outcomes of sinus surgery. *Expert Rev Respir Med.* **2012**, *6*, 493-498.

[55] Catalano, P.J.; Thong, M.; Weiss, R.; Rimash, T. The MicroFlow Spacer: A Drug-Eluting stent for the Ethmoid Sinus. *Indian J Otolaryngol Head Neck Surg.* **2011**, *63*, 279–284.

[56] Effect of Sinufoam-Dexamethasone Mixture on Post Endoscopic Sinus Surgery Outcomes. Available online: http://clinicaltrials.gov/show/NCT01024075 (accessed on 28 October 2013).

[57] Clinical Policy Bulletin: Devices for Post-Operative Use Following Endoscopic Sinus Surgery. Available online: http://www.aetna.com/cpb/medical/data/800_899/0840.html (accessed on 28 October 2013).

[58] ENT today. Drug-Eluting Sinus Stent Hits the Market: May help maintain patency after FESS. Available online: http://www.enttoday.org/details/article/1420005/Drug-Eluting_Sinus_Stent_Hits_the_ Market_May_help_maintain_patency_after_FESS.html (accessed on 10 August 2013).

[59] Newsletters: New ethmoid spacer for drug delivery. Available online: https://med.uth.edu/orl/newsletter/ethmoid-spacer-drug-delivery/ (accessed on 19 May 2014)

[60] Implantable sinus stents for postoperative use following endoscopic sinus surgery. Available online: https://www.premera.com/medicalpolicies/cmi_136631.htm (accessed on 16 March 2014).

[61] U.S. Food and Drug Administration. Maude adverse event report: acclarent, inc.relieva stratus microflow spacer stratus ethmoid spacer**.** Available online: http://www.accessdata.fda.gov/scripts/cdrh/cfdocs/cfMAUDE/detail.cfm?mdrfoi__id=1461307 (accessed on 15 January 2014).

[62] Acclarent. Instructions for use. Available online: https://www.jnjgatewayifu.com/eLabelingContent/Acc/USENG/IFU005013_Rev_F_Stratus_81590.pdf (accessed on 18 March 2014).

[63] Available online: http://www.ich.org/fileadmin/Public_Web_Site/ICH_Products/Guidelines/Quality/Q2_R1/Step4/Q2_R1__Guideline.pdf (accessed on 17 February 2014).

[64] Khaled, K.A.; Sarhan, H.A.; Ibrahim, M.A.; Ali, A.H.; Naguib, Y.W. Prednisolone-loaded PLGA microspheres. in vitro characterization and in vivo application in adjuvant-induced arthritis in mice. *AAPS PharmSciTech.* **2010**, 11, 859-869.

[65] Ju, Y.M.; Yu, B.; West, L.; Moussy, Y.; Moussy, F. A. Dexamethasone loaded PLGA microspheres/ collagen scaffold composite for implantable glucose sensors. *J Biomed Mater Res A*. **2010**, *93*, 200-210.

[66] Fan, M.; Guo, Q.; Luo, J.; Luo, F.; Xie, P.; Tang, X.; Qian, Z. Preparation and *in vitro* characterization of dexamethasone-loaded poly(D,L-lactic acid) microspheres embedded in poly(ethylene glycol)-poly({varepsilon}-caprolactone)-poly(ethylene glycol) hydrogel for orthopedic tissue engineering. *J Biomater Appl.* **2013**, *28*, 288-297.

[67] Herrera, L.C.; Tesoriero, M.V.D.; Hermida, L.G. *In vitro* Release Testing of PLGA Microspheres with Franz Diffusion Cells. Available online: http://www.dissolutiontech.com/DTresour/201205Articles/DT201205_A01.pdf (accessed on 05 February 2014).

[68] Mekhail, M.; Daoud, J.; Almazan, G.; Tabrizian, M. Rapid, guanosine 5'-diphosphate-induced, gelation of chitosan sponges as novel injectable scaffolds for soft tissue engineering and drug delivery applications. *Adv Healthc Mater.* **2013**, 2, 1126-1130.

[69]Alvarez-Fuentes, J.; Martín-Banderas, L.; Muñoz-Rubio, I.; Holgado, M.A.; Fernández-Arévalo, M. Development and validation of an RP-HPLC method for CB13 evaluation in several PLGA nanoparticle systems. *Scientific World Journal*. **2012**.

[70] Liu, H.; Slamovich, E.B.; Webster, T.J. Less harmful acidic degradation of poly(lactic-co-glycolic acid) bone tissue engineering scaffolds through titania nanoparticle addition. *Int J Nanomedicine.* **2006,** 1, 541-545.

[71] Shive, M.S.; Anderson, J.M. Biodegradation and biocompatibility of PLA and PLGA microspheres. *Adv Drug Deliv Rev.* **1997,** 28, 5-24.

[72] Kemala, T.; Budianto, E.; Soegiyono, B. Preparation and characterization of microspheres based on blend of poly(lactic acid) and poly(ε-caprolactone) with poly(vinyl alcohol) as emulsifier. *Arabian J Chemistry.* **2010,** 5, 103-108.

[73] Jelvehgari, M.; Nokhodchi, A.; Rezapour, M.; Valizadeh, H. Effect of formulation and processing variables on the characteristics of tolmetin microspheres prepared by double emulsion solvent diffusion method. *Indian J Pharm Sci.* **2010**, 72, 72-78.

[74] Sahoo, S.K.; Panyam, J.; Prabha, S.; Labhasetwar, V. Residual polyvinyl alcohol associated with poly (D,L-lactide-co-glycolide) nanoparticles affects their physical properties and cellular uptake. *J Control Release.* **2002**, 82, 105-114.

[75] Faisant, N.; Siepmann, J.; Benoit, J.P. PLGA-based microparticles: elucidation of mechanisms and a new, simple mathematical model quantifying drug release. *Eur J Pharm Sci.* **2002**, 15, 355-366.

[76] Meulemans, W.; De Loof, A. Transport of the cationic fluorochrome rhodamine 123 in an insect's Malpighian tubule: indications of a reabsorptive function of the secondary cell type. *J Cell Sci.* **1992**, 101, 349-361.

[77] Shao, D.; Massoud, E.; Anand, U.; Parikh, A.; Cowley, E.; Clarke, D.; Agu, R.U. Organic cation transporters in human nasal primary culture: expression and functional activity. *Ther Deliv.* **2013**, 4, 439-451.

[78] Nies, A.T.; Koepsell, H.; Damme, K.; Schwab, M. Organic cation transporters (OCTs, MATEs), *in vitro* and *in vivo* evidence for the importance in drug therapy. *Handb Exp Pharmacol.* **2011**, 201, 105 – 167**.**

[79] Krester, M.; Karpa, K.D.; Vrana, K.E. Elsevier's integrated review pharmacology. 2nd edition. Available online: https://www.inkling.com/read/elseviers-integrated-review-pharmacology-kester-karpa-vrana-2nd/chapter-1/absorption (accessed on 20 May 2014).

[80] Roerig, D.L.; Audi, S.H.; Ahlf, S.B. Kinetic characterization of P-glycoprotein-mediated efflux of rhodamine 6G in the intact rabbit lung. *Drug Metab Dispos.* **2004**, 32, 953-958.

[81] Derakhshandeh, K.; Hochhaus, G.; Dadashzadeh, S. In-vitro cellular uptake and transport study of 9-nitrocamptothecin PLGA nanoparticles across Caco-2 Cell monolayer model. *Iran J Pharm Res.* **2011**, 10, 425-434.

[82] Ali Khan, A.; Mudassir, J.; Mohtar, N.; Darwis, Y. Advanced drug delivery to the lymphatic system: lipid-based nanoformulations. *Int J Nanomedicine.* **2013**, 8, 2733-2744.

[83] Desai, M.P.; Labhasetwar, V.; Walter, E.; Levy, R.J.; Amidon, G.L. The mechanism of uptake of biodegradable microparticles in Caco-2 cells is size dependent. *Pharm Res.* **1997**, 14, 1568-1573.

[84] Bleier, B.S.; Paulson, D.P.; O'Malley, B.W.; Li, D.; Palmer, J.N.; Chiu, A.G.; Cohen, N.A. Chitosan glycerophosphate-based semirigid dexamethasone eluting biodegradable stent. *Am J Rhinol Allergy.* **2009**, 23, 76-79.

[85] Perez, A.C.; Cunha Junior Ada, S.; Fialho, S.L.; Silva, L.M.; Dorgam, J.V.; Murashima Ade, A.; Silva, A.R.; Rossato, M.; Anselmo-Lima, W.T. Assessing the maxillary sinus mucosa of rabbits in the presence of biodegradable implants. *Braz J Otorhinolaryngol*. **2012**, 78, 40-46.